Journal of Innate Immunity

Research Article

J Innate Immun 2024;16:262–282
DOI: 10.1159/000538364

Received: September 17, 2023
Accepted: March 12, 2024
Published online: April 24, 2024

Stat3 Regulates Developmental Hematopoiesis and Impacts Myeloid Cell Function via Canonical and Non-Canonical Modalities

Mohamed Luban Sobah[a] Clifford Liongue[a, b] Alister C. Ward[a, b]

[a]School of Medicine, Deakin University, Geelong, VIC, Australia; [b]Institute of Mental and Physical Health and Clinical Translation (IMPACT), Deakin University, Geelong, VIC, Australia

Keywords
Animal models · Cytokines · Granulocyte colony-stimulating factor · Innate immunity · Macrophage · Neutrophil · STAT3 · Zebrafish

Abstract
Introduction: Signal transducer and activator of transcription (STAT) 3 is extensively involved in the development, homeostasis, and function of immune cells, with STAT3 disruption associated with human immune-related disorders. The roles ascribed to STAT3 have been assumed to be due to its canonical mode of action as an inducible transcription factor downstream of multiple cytokines, although alternative noncanonical functional modalities have also been identified. The relative involvement of each mode was further explored in relevant zebrafish models. ***Methods:*** Genome editing with CRISPR/Cas9 was used to generate mutants of the conserved zebrafish Stat3 protein: a loss of function knockout (KO) mutant and a mutant lacking C-terminal sequences including the transactivation domain (ΔTAD). Lines harboring these mutations were analyzed with respect to blood and immune cell development and function in comparison to wild-type zebrafish. ***Results:*** The Stat3 KO mutant showed perturbation of hematopoietic lineages throughout primitive and early definitive hematopoiesis. Neutrophil numbers did not increase in response to lipopolysaccharide (LPS) or granulocyte colony-stimulating factor (G-CSF) and their migration was significantly diminished, the latter correlating with abrogation of the Cxcl8b/Cxcr2 pathway, with macrophage responses perturbed. Intriguingly, many of these phenotypes were not shared by the Stat3 ΔTAD mutant. Indeed, only neutrophil and macrophage development were disrupted in these mutants with responsiveness to LPS and G-CSF maintained, and neutrophil migration actually increased. ***Conclusion:*** This study has identified roles for zebrafish Stat3 within hematopoietic stem cells impacting multiple lineages throughout primitive and early definitive hematopoiesis, myeloid cell responses to G-CSF and LPS and neutrophil migration. Many of these roles showed conservation, but notably several involved noncanonical modalities, providing additional insights for relevant diseases.

Introduction

Mammals possess seven signal transducer and activator of transcription (STAT) proteins that are responsible for regulating a myriad of key cellular processes, such as differentiation, proliferation, survival, and functional activation [1]. STAT3 is considered an oncogene, being hyperactivated in a large variety of human cancers acting as a potent transcription factor within malignant cells [2, 3], as well as being involved in the

karger@karger.com
www.karger.com/jin

Correspondence to:
Alister C. Ward, award@deakin.edu.au

regulation of antitumor immunity [4–6]. Somatic gain-of-function (GOF) STAT3 mutations have also been linked to the development of large granular lymphocytic (LGL) leukemias and multisystem primary immune regulatory syndromes, with most patients also showing signs of autoimmunity [7, 8]. Alternatively, germline loss-of-function (LOF) STAT3 mutations have been implicated in the development of autosomal dominant hyper-IgE syndrome (AD-HIES), which has similar symptoms to those caused by GOF mutations, with recurrent infections and autoimmunity [9, 10]. Various pharmacological inhibitors that inhibit STAT3 activation have proven efficacious in diseases associated with hyperactivation or GOF mutations [11]. However, the mechanisms underlying disease etiology in the context of LOF STAT3 mutations remain poorly understood, meaning current treatments primarily focus on the alleviation of symptoms rather than rectifying the underlying cause [12–14].

Global STAT3 knockout (KO) mice exhibited embryonic lethality, primarily due to disrupted leukemia inhibitory factor (LIF) signaling that impacted embryonic stem cells [15], which has limited the study of STAT3 to particular cell lineages using conditional mouse KOs [16]. Ablation of STAT3 in hematopoietic progenitor cells allowed survival to 4–6 weeks, but these mice ultimately succumbed to prolonged systemic inflammation reminiscent of Crohn's disease [17]. Ablation of STAT3 in lymphocytes revealed specific roles in the differentiation of $CD4^+$ T cells, particularly towards the Th17 subset, largely due to impacts on IL-6 and IL-21 signaling [18, 19]. Ablation of STAT3 directly impacted early B-cell development [20], while B-cell maturation was indirectly affected following STAT3 ablation in T follicular helper cells [21]. Myeloid-specific ablation of STAT3 identified a role in the polarization of macrophages in response to infection [22] and a more prominent role in neutrophils, particularly in response to emergency situations such as bacterial infection or injury [23–25]. These roles have been ascribed to the canonical mode of STAT function as inducible transcription factors downstream of cytokine and other receptors, although several noncanonical modes of STAT function have also been identified that require consideration [26].

Zebrafish STAT3 is highly conserved with its mammalian counterparts [27], and is expressed in similar lineages and activated downstream of conserved pathways suggesting significant conservation of function. However, in contrast to mice, zebrafish harboring Stat3 KO mutations have been shown to survive embryogenesis, allowing functional studies into the juvenile stage [28, 29]. This has been exploited in this study that investigates two different Stat3 mutants: a Stat3 KO mutant and a C-terminal truncation mutant impacting the transactivation domain (ΔTAD) that mimics human STAT3 LOF mutations [9, 30]. These have been thoroughly characterized with respect to primitive and early definitive hematopoiesis, as well as neutrophil and macrophage functionality. This has identified important contributions to immune cell development and function, with both canonical or non-canonical modes of action likely involved, which has implications for human disease.

Materials and Methods

Zebrafish Husbandry

Wild-type (WT) zebrafish and the transgenic lines Tg(*mpx*:GFP)^{i114} [31] and Tg(*mpeg1.1*:GFP)^{gl22} [32] were maintained in accordance with standard husbandry practices in a purpose-built Techniplast aquarium on a 14/10 h light/dark cycle with thrice daily feeding. Embryos were maintained at 28.5°C in E3 water up to 24 h post fertilization (hpf) when this was replaced with 0.003% (w/v) 1-phenyl-2-thio-urea (PTU) in E3 water (E3/PTU) to inhibit pigmentation and promote transparency.

Genetic Manipulation and Line Generation

Single guide RNAs (sgRNAs) were designed against the zebrafish *stat3* gene (Acc. No. NM_131479.1) using CHOPCHOP v3 [33] targeting the sequences encoding the N-terminal (sgRNA 1: 5′-GGTGCTGCTTGATGCGCCGC) or SH2 (sgRNA 2: 5′-GGTAGACCAGCGGCGACACT) domains. Relevant oligonucleotides were cloned into the pDR274 expression vector as previous described [34], and the sgRNAs transcribed using a MegaShortScript™ T7 transcription kit (Thermo-Fischer Scientific) and subsequently purified with a MegaClear™ kit (Thermo-Fischer Scientific). WT embryos at the 1 cell stage were injected with ~1 nL of 1 × Danieau solution containing 12.5 ng/μL guide RNA (gRNA) and 200 ng/μL TrueCut Cas9 protein v2 (Thermo-Fischer Scientific), raised to adulthood and out-crossed with WT zebrafish. The F1 progeny were screened by high resolution melt analysis [35] and putative mutants confirmed by Sanger sequencing (Australia Genome Research Facility) of PCR products generated with primers flanking the respective sgRNA target sites (Table 1). Zebrafish carrying suitable mutant alleles were further out-crossed with WT zebrafish.

Experimental Setup

Experiments were performed in a blinded manner with respect to genotype. Embryos derived from heterozygous in-crosses of each mutant were pooled, with samples genotyped post-analysis. Each experiment was repeated three times. For embryos subjected to WISH, genomic DNA was extracted using a genomic lysis buffer (12.5 mM Tris [pH 8.3], 62.5 mM KCl, 1.875 mM $MgCl_2$, 0.0042% [v/v] Tween 20, 0.0042% [v/v] nonylphenoxy polyethoxy ethanol

Table 1. Primers used for PCR applications related to mutant screening and confirmation

Mutation	Application	Primers	Reference
stat3 KO	Genomic PCR/HRM	F: 5′-CCAACAAGGAGTCTCACGCC R: 5′-GGGCTTCTCCAGATACTTGC	This paper
stat3 KO	Genomic PCR/sequencing	F: 5′-CCAACAAGGAGTCTCACGCC R: 5′-CAGTAGACGCTGCTCTTCCCAC	This paper
stat3 KO	RT-PCR/sequencing	F: 5′-GTTTCCGTGGAGGACGATTTA R: 5′-AGTGGGATGGGCAACCTGG	This paper
stat3 ΔTAD	Genomic PCR/HRM	F: 5′-TGAGATCATCATGGGCTACAA R: 5′-TGTCAGGGAACTCAGTGTCT	This paper
stat3 ΔTAD	Genomic PCR/sequencing	F: 5′-CCAGATTCAGTCGGTTG R: 5′-TGTCAGGGAACTCAGTGTCT	This paper
stat3 ΔTAD	RT-PCR/sequencing	F: 5′-GAGAGAGAGCAATCCTGAGTCC R: 5′-CTAACTCTGGCAACACAAGCG	This paper

HRM, high-resolution melt.

[NP40]), as previously described [36]. For all other embryos or samples, genotyping was performed using QuickExtract (Bioline), according to the manufacturer's protocol.

Whole Mount in situ Hybridization

Zebrafish embryos were fixed with 4% (w/v) paraformaldehyde in PBS-T at 4°C prior to whole-mount in situ hybridization using DIG-labeled antisense probes, as previously described [37].

In vivo Analysis

Transgenic embryos at 3 dpf were injected into the venous return with 100 ng/μL lipopolysaccharide (LPS) (#00-4976-93, Invitrogen) in 1 × Danieau containing 1% (w/v) phenol red and incubated at 28.5°C in E3/PTU for 8 h, followed either by imaging or RNA extraction. Alternatively, 100 ng/μL mRNA encoding the zebrafish granulocyte colony-stimulating factor (G-CSF) paralogue, Csf3a, in 1 × Danieau buffer containing 1% (w/v) phenol red was injected into 1 cell stage embryos [38] with imaging or RNA extraction performed at 3 dpf. Neutrophil and macrophage migration was assessed using a wound healing assay [39]. Transgenic embryos at 3 dpf were anaesthetized with 5 μg/mL benzocaine in E3/PTU before the excision of their caudal fin, with the injury site imaged at 4 h intervals using fluorescence microscopy.

Gene Expression Analysis

Total RNA was extracted from juvenile zebrafish with TRIsure (Bioline), according to the manufacturers' protocols. Single zebrafish embryos were euthanized and homogenized in RLT buffer (Qiagen) using a TissueLyser II (Qiagen) for subsequent RNA extractions with the RNeasy Mini Kit (Qiagen), according to the manufacturer's protocols for extracting RNA from low sample volumes. For tail wounding assays, whole embryos were used since RNA yield from isolated tails was low and variable. Extracted RNA was subjected to quantitative real-time reverse-transcription PCR (qRT^2-PCR) with gene-specific primers (Table 2). Data were normalized relative to *actb* and fold-change calculated using the ΔCT method [47]. Alternatively, RT-PCR was performed with different primes (Table 1), followed by gel electrophoresis and sequencing of isolated products.

Imaging and Image Analysis

Imaging was performed on an Olympus MVX10 microscope using either standard lighting or UV excitation coupled with a GFP filter for transgenic embryos. Images were captured with a DP74 camera using CellSens Dimension 1.6 software (Olympus). The relative area of staining or fluorescence was measured using ImageJ while specific cell populations were quantified by manual counting, including the number of cells in each quadrisect of the yolk relative to the total number of cells during development. Cell numbers for the wounding assay were manually determined using the images from each timepoint, as previously described [39]. Total cell numbers at each timepoint were normalized with respect to the total average cell population of the respective genotype. The rate of cell migration was calculated by dividing the net number of cells migrating to the site of injury by the time taken to reach the peak. Alternatively, the rate of egress was calculated using the decline of cells from the peak to 24 h divided by the time between these points.

Statistics

Statistical analyses were performed using Graph Pad Prism version 8. Normality of data was tested using the D'Agostino-Pearson omnibus normality test and unequal variances using the *F* test. The difference between more than two groups was tested for significance using ordinary one-way ANOVA coupled with Tukey's multiple comparison test. In cases where there were multiple variables with more than two groups, a two-way ANOVA with Tukey's multiple comparison test was performed. If data did not follow a normal distribution, the Mann-Whitney U test was performed. In cases where two groups required comparisons, a Student's *t* test was performed with Welch's correction if variances

Table 2. Primers used for quantitative real-time reverse-transcription PCR/RT-PCR

Gene	Accession number	Primers	References
actb	NM131031	F: 5′-TGGCATCACACCTTCTAC R: 5′-AGACCATCACCAGAGTCC	[40]
cd4-1	NM_001135096	F: 5′-CTACCCAGAGAAAAGATTGAACG R: 5′-AGAAATCTGCTGATAGAGAGACG	[39]
cd8a	NM_001040049	F: 5′-ACTCTTCTTCGGAGAGGTGAC R: 5′-ACAGGCTTCAGTGTTGTTTGAA	[41]
csf1a	NM_001114480.1	F: 5′-ACGTCTGTGGACTGGAACTG R: 5′-CTGTTGGACAAATGCAGGGG	[42]
csf1b	NM_001080076.1	F: 5′-GGATTTGGGTCGGTGAGCTT R: 5′-TGGAGAGGGGAACACACAGT	[42]
csf3a	NM_001145242.1	F: 5′-CTACTGGAGTCTGGTGATTGGC R: 5′-CGTTGTGTCTGCTCCTGTTCC	This paper
csf3b	NM_001143754	F: 5′-GTGTGCAGCGGATGCTCAT R: 5′-CTGCGAGGTCGTTCAGTAGGTT	[39]
csf3r	NM_001113377.1	F: 5′-CAACCACACACTAAATATCATGCCC R: 5′-GTGACCTTCTTGCTGCGAGGCGAC	[41]
cxcl8a	XM_009306855	F: 5′-CCAGCTGAACTGAGCTCCTC R: 5′-GGAGATCTGTCTGGACCCCT	[43]
cxcl8b	NM_001327985.1	F: 5′-GCTGGATCACACTGCAGAAA R: 5′-TCAAGGAAAAGTTTGCAGCA	[43]
cxcr1	–	F: 5′-TTCAGTTCGGCTGCACTATG R: 5′-GGAGCAACTGCAGAAACCTC	[44]
cxcr2	XM_017357899.2	F: 5′-TGACCTGCTTTTTTCCCTCACT R: 5′-TGACCGGCGTGGAGGTA	[44]
epor	NM_001043334.1	F: 5′-GTCAGATACGCTGTGGAGGGA R: 5′-TCACAGGACTGGTCCAAAA	This paper
fcer1gl	XM_021478398.1	F: 5′-TGGTGCTGATGAAGATCTTC R: 5′-GGCGGATTTCATCTTGATGC	This paper
hbaa1.1	NM_131257	F: 5′-GGGAGGTCTTGAGAGAGCC R: 5′-GCAATCAGCGAGAAGCCTGA	[45]
ighd	XM_0.21474792.1	F: 5′-CGATTGTGTTGGATTCAGCCC R: 5′-GACCAACAACAAGTCCGAG	This paper
ighm	AF281479	F: 5′-AAAGATTTGAGCGATTTTGTGC R: 5′-GCTAAACACATGAAGGTTGCTG	[39]
ikzf1	NM_130986	F: 5′-AAGCGAAGTCACACTGAAGAAAG R: 5′-CAGATGTCCAGTGAGAGCGTC	[39]
il4	NM_001170740	F: 5′-CTGAATGGGAAAGGGGAAA R: 5′-CGAGAAACTCCTTCATTGTGC	[39]
il6	NM_001261449	F: 5′-TCAGAGACGAGCAGTTTGAGAGAG R: 5′-GTTAGACATCTTTCCGTGCTG	[39]
il13	NM_001199905.1	F: 5′-GCCTTCAGACCACTAATCTTTTG R: 5′-ACTTGGTCTTGGGCTTTTTTG	This paper
il21	NM_001128574	F: 5′-GAACTCAAGAAGATTCAGCAGG R: 5′-GTTCGGCTGTTGACCATTG	[39]
mmp9	NM_213123.1	F: 5′-ACTCTCCTTTGAGGACCACC R: 5′-GCTTTCGGTGGAGTGCCC	This paper

Table 2 (continued)

Gene	Accession number	Primers	References
mpeg1.1	NM_212737	F: 5′-GTTACAGCACGGGTTCAA R: 5′-TGTTTTCAATGGCGTCAGC	[39]
mpx	NM_001351837	F: 5′-CTGCGGGACCTTACTAATGATGG R: 5′-CCTGGATATGGTCCAAGGTGTC	[46]
nklc	NM_001311793.1	F: 5′-TGTGCTGCTCACTTGGAGATGC R: 5′-CATAGTCCAGGCAGTTGTTCC	[39]
scl	NM_213237	F: 5′-GCTTTCCCTCTCCCGGCACG R: 5′-GTTCGTGAAAATCCGTCGCA	[39]
socs3b	NM_213304.1	F: 5′-GGATGTGGAAGAAGTGTCAGAGCT R: 5′-GCCGTTTTCACACTGAGCGT	This paper
stat3	NM_131479.1	F: 5′-TGATGCCTCTCTGATAGTG R: 5′-GAGTGCGTCTCAAGGTCG	This paper
tcra	AF425590	F: 5′-ACTGAAGTGAAGCCGAAT R: 5′-CGTTAGCTCATCCACGCT	[39]

were unequal. Survival was visualized on a Kaplan-Meier graph, with the Gehan-Breslow-Wilcoxon test used to compare between different groups.

Results

Generation of stat3 Zebrafish Mutants

To produce relevant Stat3 mutants, two separate sgRNAs were designed to target the zebrafish *stat3* gene: sgRNA 1 for exon 3, encoding the N-terminal domain, and sgRNA 2 for exon 20, encoding the C-terminal portion of the SH2 domain (Fig. 1a). The sgRNAs were injected separately with Cas9 protein into WT embryos, which were then raised to adulthood and out-crossed with WT fish. Screening of F1 progeny identified one allele from each sgRNA that impacted the corresponding Stat3 reading frame. Zebrafish carrying these alleles were out-crossed again, with heterozygous carrier progeny of each allele in-crossed to produce homozygous F3 mutants. Sequence analysis revealed that the sgRNA 1-generated allele (*ko*/*mdu35*) was a 4 bp deletion that resulted in a frameshift and premature stop codon, leading to a severely truncated Stat3 protein representing a loss-of-function KO mutation (Fig. 1b, d). The allele generated from sgRNA 2 (*Δtad*/*mdu36*) was an 8 bp deletion that also resulted in a frameshift mutation and early stop codon just after the last binding pocket of the SH2 domain causing the complete truncation of the TAD (ΔTAD) (Fig. 1c, d). Gel electrophoresis and sequence analysis of RT-PCR products confirmed the presence of the respective deletions in the transcribed mRNA, with no apparent change to splicing evident, and also revealed lower *stat3* transcript levels in both mutants (online suppl. Fig. 1; for all online suppl. material, see https://doi.org/10.1159/000538364).

To further elucidate the roles of Stat3 within the neutrophil and macrophage lineages both mutant lines were crossed onto the Tg(*mpx*:GFP) [48] and Tg(*mpeg1.1*:GFP) [32] transgenic backgrounds that mark neutrophils and macrophages, respectively. In subsequent experiments, mutants were compared to those encoding WT Stat3.

Stat3 Contributes to Primitive Hematopoiesis and Migration of Primitive Neutrophils

The effect of the two Stat3 mutations on primitive hematopoiesis was investigated using WISH with lineage-specific markers at relevant timepoints (12 hpf, 16 hpf, and 22 hpf). Compared to the Stat3 WT, KO embryos were found to have a significantly diminished population of early hematopoietic progenitor cells identified using a probe specific for the *scl* gene [49] at 12 hpf both caudally (Fig. 2a–d) and rostrally (Fig. 2e–h). A similar effect was seen with the early erythroid (Fig. 2i–l) and myeloid (Fig. 2m–p) populations stained with *gata1a* [50] and *spi1b* [40], respectively. This extended to mature erythroid cells stained with *hbbe1.1* [51] (Fig. 2q–t), neutrophils stained with *mpx* [52] (Fig. 2u–x) and *csf3r* [38]

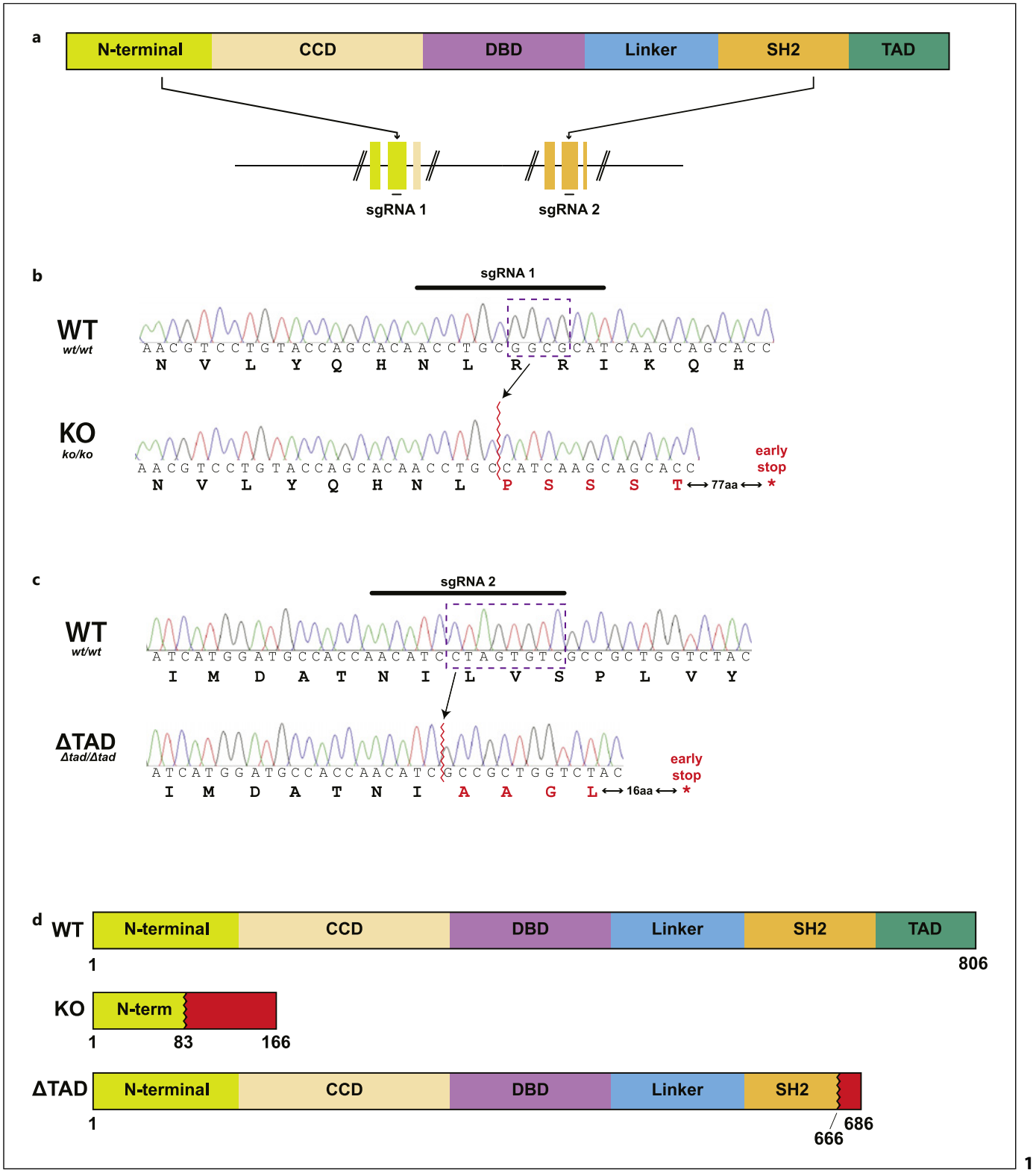

1

(For legend see next page.)

(Fig. 2y–b′) and fluorescently marked macrophages in the Tg(*mpeg1.1*:GFP) line [32] (Fig. 2c′–f′). In contrast, ΔTAD mutants did not show any alteration in early hematopoietic progenitor cells (Fig. 2a–h), early erythroid cells (Fig. 2i–l), early myeloid (Fig. 2m–p) cells or mature erythroid cells (Fig. 2q–t). However, both neutrophil populations (Fig. 2u–x and Fig. 2y–b′) and macrophages (Fig. 2c′–f′) were significantly decreased in ΔTAD mutants compared to WT, although the neutrophil populations remained significantly higher than in KO mutants (Fig. 2u–b′).

As part of normal development, primitive neutrophils and macrophages migrate across the yolk sac [38]. KO embryos exhibited reduced migration of neutrophils marked with *mpx* (Fig. 2u–w) and *csf3r* (Fig. 2y–a′) compared to WT embryos. Closer examination of KO embryos revealed the majority of *mpx*$^+$ and *csf3r*$^+$ cells had migrated less than one quarter of the way across the yolk compared to those in WT embryos that had migrated to a greater extent across the yolk (online suppl. Fig. 2A–H). In contrast, ΔTAD embryos resembled the WT (Fig. 2u–w; Fig. 2y–a′; online suppl. Fig. 2A–H). No impact on macrophage migration was evident in either mutant (Fig. 2c′–e′).

Stat3 Is Important in Innate Immune Cell Production during Definitive Hematopoiesis

The effect of the Stat3 mutations on definitive hematopoiesis was also investigated using WISH at 3–5 dpf. Hematopoietic stem cells stained with *cmyb* [53] were significantly diminished in Stat3 KO mutants both caudally (Fig. 3a–d) and rostrally (Fig. 3e–h). Similarly KO mutants showed a marked decrease in lymphoid precursor cells stained with *ikzf1* [54] (Fig. 3i–l) as well as mature lymphoid cells stained with *rag1* [55] (Fig. 3m–p) and *tcra* [56] (Fig. 3q–t) and mature erythrocytes stained with *hbbe1.1* (Fig. 3u–x). Neutrophils stained with *mpx* (Fig. 3y–b′) or *csf3r* (Fig. 3c′–f′) as well as *mpeg1.1*$^+$ macrophages (Fig. 3g′–j′) were all significantly reduced in KO mutants. In contrast, the ΔTAD mutants did not show any alterations in hematopoietic stem cells (Fig. 3a–h), lymphoid precursor cells (Fig. 3i–l), lymphoid cells (Fig. 3m–t), or mature erythroid cells (Fig. 3u–x). However, both neutrophil populations (Fig. 3y–b′; Fig. 3c′–f′) and macrophages (Fig. 3g′–j′) were all significantly reduced compared to the WT, although the macrophage population remained significantly higher than the KO mutants (Fig. 3g′–j′).

Stat3 Plays a Role in the Innate Immune Response to Injury

To further explore the functional impacts of the Stat3 mutations on neutrophils and macrophages, embryos derived from the Stat3 mutants on either the Tg(*mpx*:GFP) or Tg(*mpeg1.1*:GFP) transgenic backgrounds were subjected to a caudal fin wounding assay at 3 dpf (Fig. 4a). The Stat3 KO embryos exhibited a marked decrease in the total number of neutrophils migrating to the injury site compared to WT embryos (Fig. 4b–c). However, when these data were normalized to the overall *mpx*$^+$ cell number in the embryos, no significant difference in the proportion of neutrophils migrating was evident (Fig. 4d). Further analysis revealed a significant decrease in the migration rate (online suppl. Fig. 3C), but the cell size (online suppl. Fig. 3A) and egress rate (online suppl. Fig. 3E) were not impacted. No difference was observed in the number of total macrophages migrating (Fig. 4e–f) but normalization revealed that KO embryos had an increased proportion of macrophages migrating compared to WT embryos (Fig. 4g). Interestingly, the size of the macrophages was decreased in KO embryos (online suppl. Fig. 3B), but the rate of migration (online suppl. Fig. 3D) and egress (online suppl. Fig. 3F) were not affected. The ΔTAD mutant did not show any alteration in the number of neutrophils (Fig. 4e, f) or macrophages (Fig. 4b, c) recruited to the injury site. However, when normalized to overall cell counts the ΔTAD mutants showed a higher proportion of neutrophils migrating compared to both WT and KO mutant embryos (Fig. 4d) and of macrophages migrating compared to WT embryos (Fig. 4g). No change was observed in the size (online suppl. Fig. 3A), rate of migration (online suppl. Fig. 3C) or egress (online suppl. Fig. 3E) of neutrophils or the size (online suppl. Fig. 3B), rate of migration (online suppl. Fig. 3D) or egress (online suppl. Fig. 3F) of macrophages in ΔTAD mutants.

Fig. 1. Generation of zebrafish Stat3 mutants. Schematic of the STAT3 protein outlining the various functional domains: N-terminal, CCD (coiled-coil domain), DBD (DNA binding domain), linker, SH2 (Src homology 2 domain), and TAD (transactivation domain), along with relevant sections of the zebrafish *stat3* gene showing introns (black lines) and exons (colored boxes) encoding the indicated protein domains as well its targeting by sgRNAs (**a**). Sequence traces of representative homozygous wild-type (WT, *stat3*$^{wt/wt}$) and knockout (KO, *stat3*$^{ko/ko}$) (**b**) and WT and transactivation domain truncation (ΔTAD, *stat3*$^{\Delta tad/\Delta tad}$) (**c**) mutant fish, with nucleotides and corresponding amino acids shown. In each case, nucleotide sequences deleted are boxed in purple with de novo amino acids in red. Schematic of Stat3 proteins expressed in WT, KO, and ΔTAD fish (**d**).

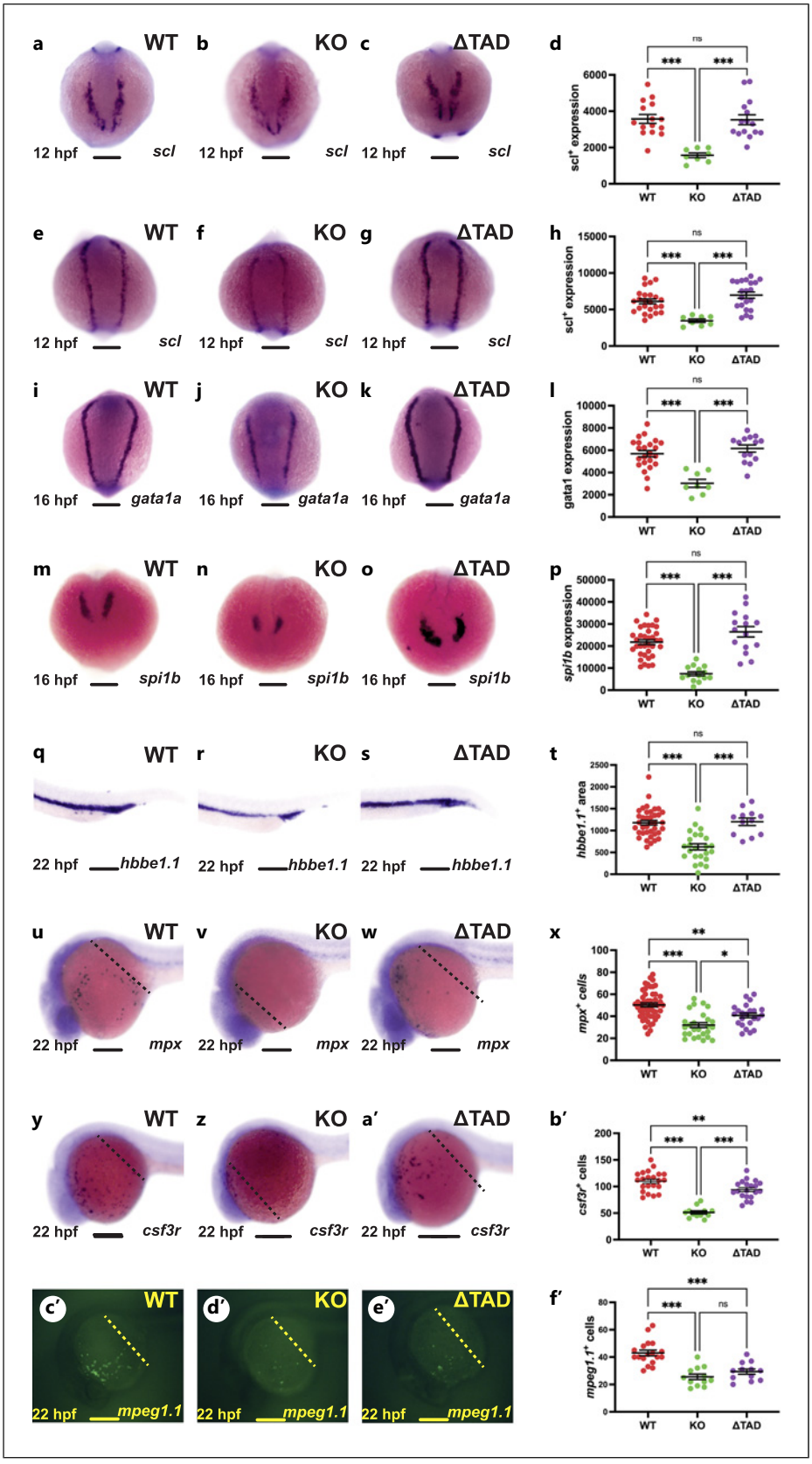

Fig. 2. Effect of Stat3 mutations on primitive hematopoiesis. Representative images of wild-type (WT), knockout (KO), and transactivation domain truncation (ΔTAD) mutant embryos subjected to WISH at 12 hpf with *scl* (**a**–**c**, **e**–**g**), at 16 hpf with *gata1a* (**i**–**k**) and *spi1b* (**m**–**o**) and at 22 hpf with *hbbe1.1* (**q**–**s**), *mpx* (**u**–**w**), and *csf3r* (**y**–**a′**) using light microscopy or those on a Tg(*mpeg1.1*:GFP) transgenic background at 22 hpf (**c′**–**e′**) using fluorescence microscopy. Scale bars represent 200 μm. Quantification of area of staining for *scl* (**d**, **h**), *gata1a* (**l**), *spi1b* (**p**), and *hbbe1.1* (**t**) and cell numbers for *mpx* (**x**), *csf3r* (**b′**), and *mpeg1.1* (**f′**) showing values for individual embryos as well as mean and SEM with statistical significance between genotypes indicated (***p < 0.001, **p < 0.01, *p < 0.05, ns: not significant).

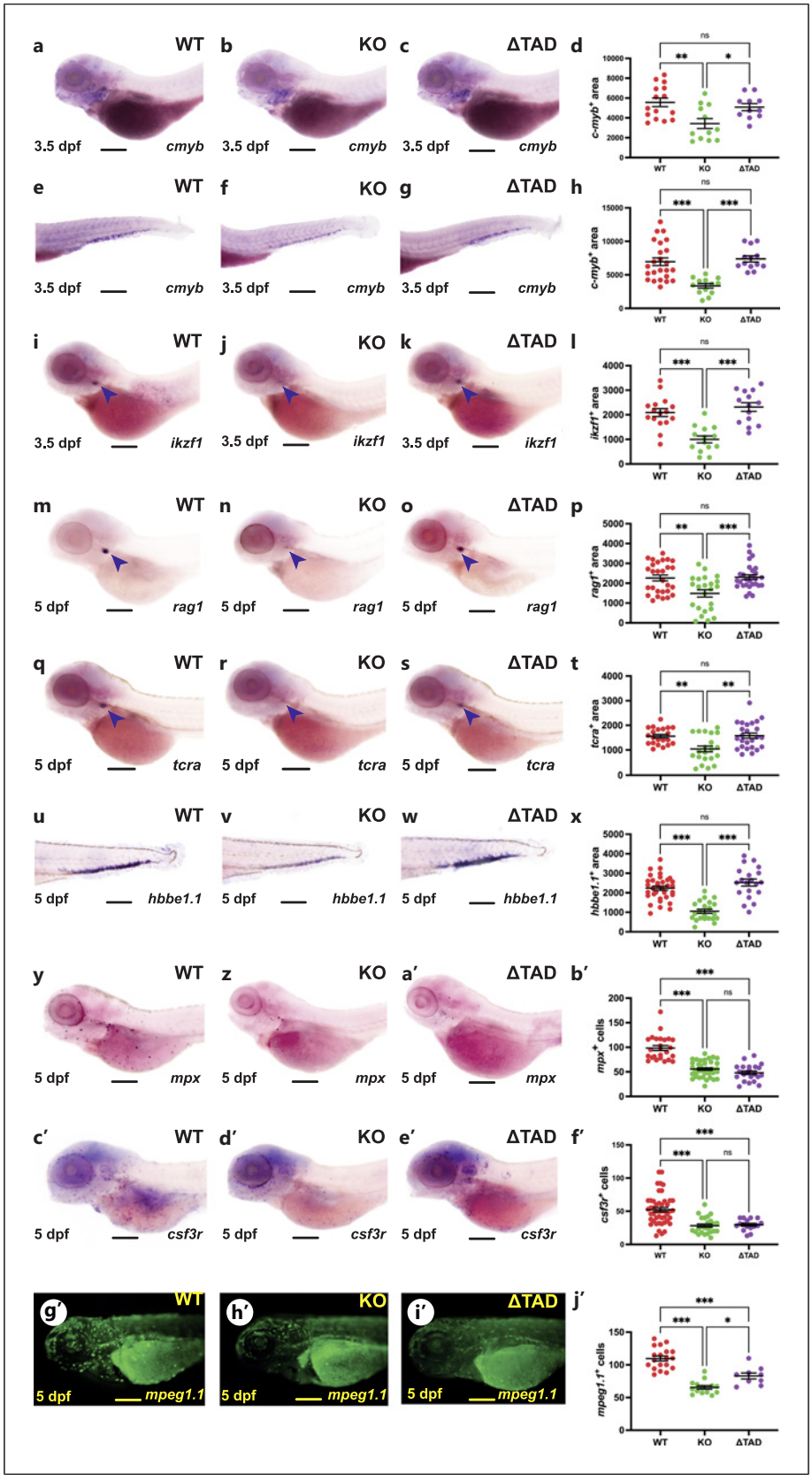

Fig. 3. Effect of Stat3 mutations on early definitive hematopoiesis. Representative images of wild-type (WT), knockout (KO), and transactivation domain truncation (ΔTAD) mutant embryos subjected to WISH at 3.5 dpf with *cmyb* (**a**–**c**, **e**–**g**) and *ikzf1* (**i**–**k**) and at 5 dpf with *rag1* (**m**–**o**), *tcra* (**q**–**s**), *hbbe1.1* (**u**–**w**), *mpx* (**y**–**a′**), and *csf3r* (**c′**–**e′**) using light microscopy or those on a Tg(*mpeg1.1*:GFP) transgenic background at 5 dpf (**g′**–**i′**) using fluorescence microscopy. Scale bars represent 200 μm. Quantification of area of staining for *cmyb* (**d**, **h**), *ikzf1* (**l**), *rag1* (P), *tcra* (**t**), and *hbbe1.1* (**x**), and cell numbers for *mpx* (**b′**), *csf3r* (**f′**), and *mpeg1.1* (**j′**) showing values for individual embryos as well as mean and SEM with statistical significance between genotypes indicated (***$p < 0.001$, **$p < 0.01$, *$p < 0.05$, ns: not significant).

J Innate Immun 2024;16:262–282
DOI: 10.1159/000538364

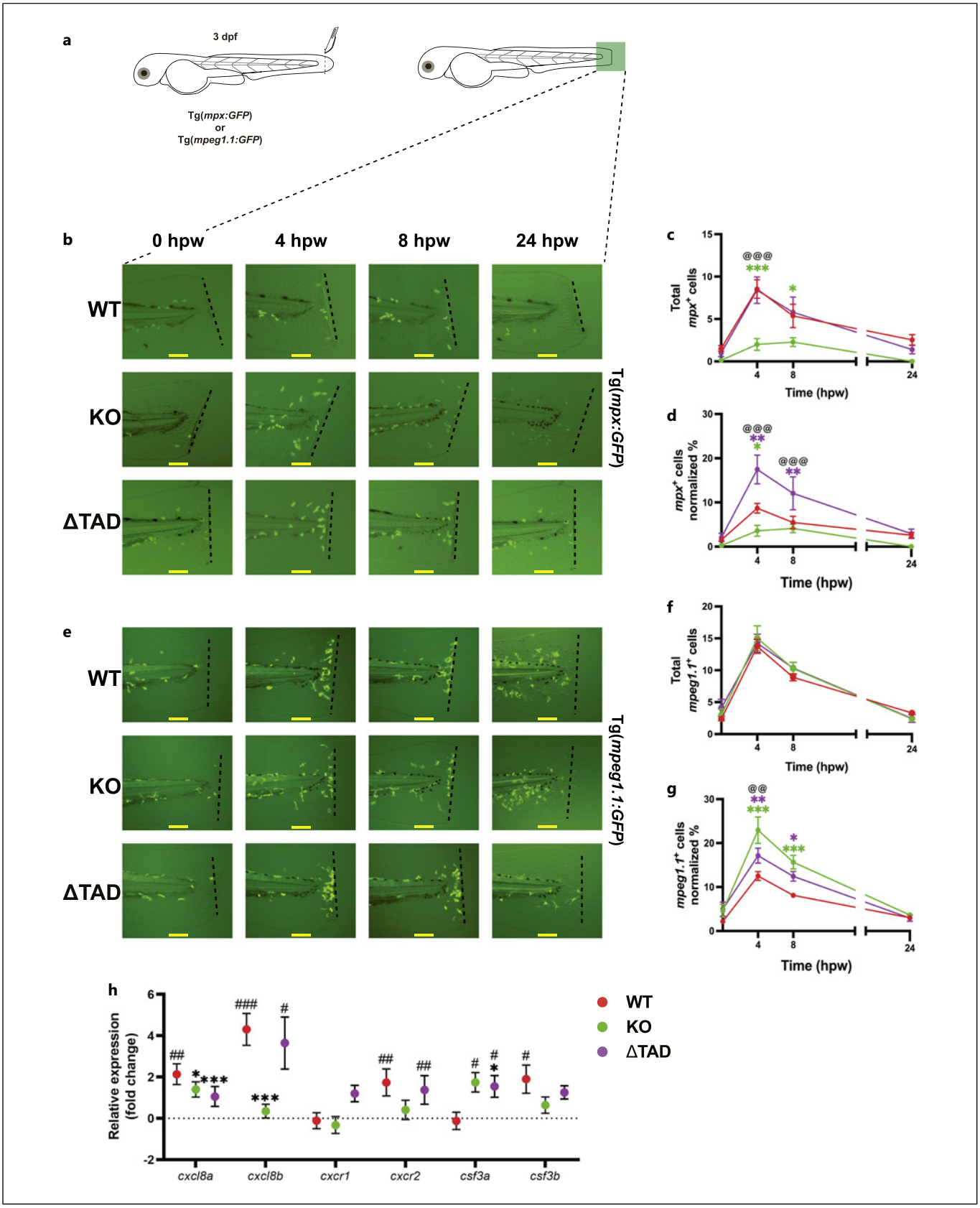

4

(For legend see next page.)

Gene expression analysis was performed at 4 h post wounding, which included genes for chemokines, *cxcl8a* and *cxcl8b* [43], and their cognate chemokine receptors, *cxcr1* and *cxcr2* [57], as well as cytokines, *csf3a* and *csf3b* [41], all implicated in neutrophil migration. Expression of *cxcl8a*, *cxcl8b*, and *cxcr2* were significantly upregulated in WT embryos in response to wounding, while KO embryos demonstrated no such change with *cxcl8a* and *cxcl8b* expression significantly reduced compared to WT following wounding (Fig. 4h). Intriguingly, *csf3b* was significantly upregulated in WT but not in KO embryos while *csf3a* was upregulated in KO but not in WT embryos in response to wounding. ΔTAD embryos exhibited a significant upregulation of *cxcr2*, *cxcl8b*, and *csf3a*, while *cxcr1*, *csf3b*, and *cxcl8a* remained unchanged in response to wounding, with significantly lower expression of *cxcl8a* and *csf3a* compared to WT following wounding.

Stat3 Is Involved in the Response to LPS

To further elucidate the impact of the Stat3 mutations on immune responses, Stat3 mutants on the Tg(*mpx*:GFP) or Tg(*mpeg1.1*:GFP) background were subjected to injection with bacterial LPS as an inflammatory mediator. WT embryos showed a significant increase in neutrophils in response to LPS injection (Fig. 5a, d, m), but such an increase was not observed in KO embryos (Fig. 5b, e, m). In contrast, a significant increase in macrophage numbers was observed in both WT (Fig. 5g, j, n) and KO (Fig. 5h, k, n) embryos, although macrophage numbers in injected KO embryos were still significantly lower than their WT counterparts (Fig. 5n). The ΔTAD mutant displayed a similar phenotype to the KO, with lower basal numbers and no change in response to LPS for neutrophils (Fig. 5c, f, m), but a significant increase in macrophage numbers in response to LPS, albeit still lower than the WT (Fig. 5i, l, n).

Expression analysis was performed in LPS-injected embryos on genes for an inflammatory cytokine, *il6* [58], as well as macrophage-specific *csf1a* and *csf1b* [59] and neutrophil specific *csf3a* and *csf3b* [41] cytokines, in addition to a negative regulator of cytokine signaling, *socs3b* [39] (Fig. 5o). LPS-injected WT embryos exhibited an upregulation of *il6*, *csf1a*, and *csf1b*, while KO embryos showed an upregulation of *il6* and *csf1b* only, with expression of *socs3b* significantly reduced in KO embryos and along with *csf3a* also compared to LPS-injected WT embryos. In contrast, LPS-injected ΔTAD embryos showed a significant increase in the expression of *csf1b* and a significant decrease in *csf3a* expression, which was also significantly decreased compared to LPS-injected WT embryos.

Stat3 Is Required for G-CSF-Mediated Emergency Granulopoiesis

The impact of Stat3 mutations on cytokine-mediated emergency granulopoiesis was assessed by injection of mRNA encoding the mammalian G-CSF paralogue, Csf3a, into embryos on the Tg(*mpx*:GFP) background. WT embryos showed a significant increase in neutrophil numbers (Fig. 6a, d, g), as described previously [38]. In contrast, KO embryos exhibited no change in neutrophil numbers in response to Csf3a injection (Fig. 6b, e, g). ΔTAD embryos, on the other hand, showed a significant increase in neutrophil numbers following Csf3a injection with numbers comparable to WT and significantly higher than Csf3a-injected KO embryos despite being comparable in uninjected embryos (Fig. 6c, f, g).

Gene expression analysis of Csf3a-injected embryos was performed for the chemokine receptor gene *cxcr2* and negative regulator *socs3b*, both shown to be induced by G-CSF through STAT3 [39, 60]. WT embryos exhibited a significant upregulation of *cxcr2* and *socs3b* in response to Csf3a injection while in KO embryos *cxcr2* was downregulated and *socs3b* remained unchanged, although both were significantly less than in Csf3a-injected WT embryos (Fig. 6h). ΔTAD embryos showed a similar response to WT embryos.

Stat3 Impacts Survival and Juvenile Immunity

Both Stat3 mutants experienced poor survival, with the KO mutants surviving less than 30 dpf, and the ΔTAD mutants less than 40 dpf, both significantly less

Fig. 4. Effect of Stat3 mutations on the response of neutrophils and macrophages to injury. Wild-type (WT), knockout (KO), and transactivation domain truncation (ΔTAD) mutant embryos on either the Tg(*mpx*:GFP) or Tg(*mpeg1.1*:GFP) transgenic background were subjected to a caudal fin wounding assay at 3 dpf and imaged using fluorescence microscopy from 0 to 24 h post wounding (hpw) (**a**). Representative images of mpx^+ neutrophil (**b**) and $mpeg1.1^+$ macrophage (**e**) cells migrating to the vicinity of the injury site (dotted line) at the indicated times, with scale bars of 100 μm. Quantitation of total migrating mpx^+ cells (**c**) or normalized relative to overall mpx^+ cells (**d**), as well as total migrating $mpeg1.1^+$ cells (**f**) or normalized relative to overall $mpeg1.1^+$ cells (**g**) ($n = 5$). Gene expression analysis of the indicated genes in WT, KO, and ΔTAD embryos ($n = 5$–6) at 4 hpw presented as fold change ($\log_2$) relative to WT (**h**). **c**, **d**, **f**–**h** show mean and SEM with statistical significance indicated compared to WT ($^{***}p < 0.001$, $^{**}p < 0.01$, $^{*}p < 0.05$), between mutants ($^{@@@}p < 0.001$, $^{@@}p < 0.01$, $^{@}p < 0.05$) or between unwounded and wounded ($^{\#\#\#}p < 0.001$, $^{\#\#}p < 0.01$, $^{\#}p < 0.05$), identified using a two-way ANOVA with Tukey's multiple comparison test.

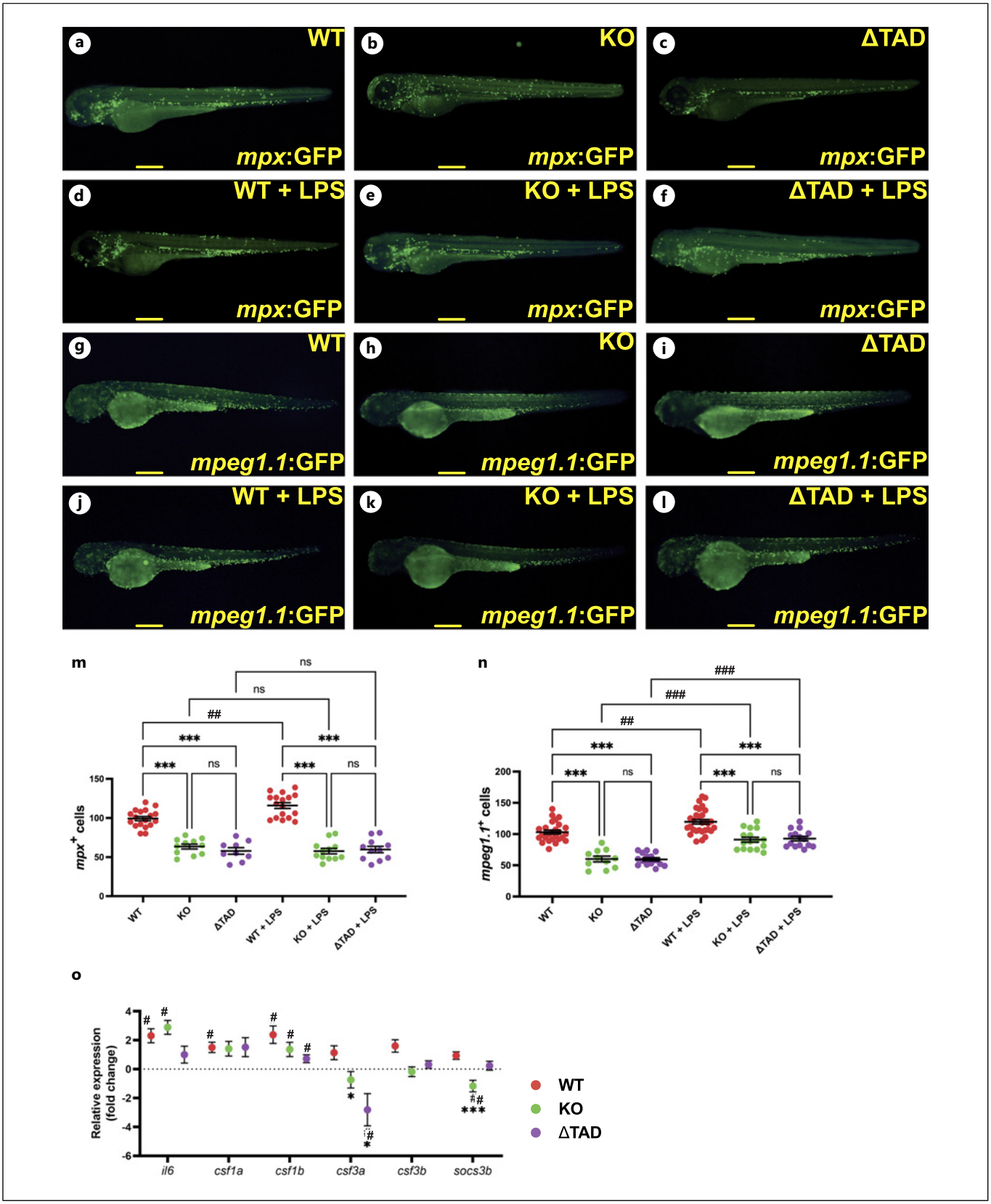

5

(For legend see next page.)

than the robust survival of WT zebrafish (Fig. 7a), consistent with alternative Stat3 KO zebrafish [28, 29]. While this precluded the study of adults, analysis of 28 dpf juvenile was possible, which enabled analysis when the full immune repertoire, including B and NK cells, was present [56, 61]. Gene expression analysis of juvenile zebrafish included a hematopoietic stem cell marker, *scl* [49], an early lymphoid marker, *ikzf1* [54], an early myeloid marker *runx1* [62], neutrophil markers, *mpx* [48], and *csf3r* [38], a macrophage marker, *mpeg1.1* [32], T-cell markers *tcra*, *cd4-1,* and *cd8a* [63], B-cell markers, *ighd*, *ighm* [64], and *fcer1gl* [65], erythrocyte markers, *hbba1* and *epor* [66], and cytokines, *il4* [67], *il13* [68], *il21*, and *il6* [69]. Compared to WT zebrafish, KO zebrafish demonstrated a significant increase in expression of the neutrophil marker *mpx*, the B-cell marker *ighm*, and the cytokine *il13*, while expression of *il6* was significantly decreased (Fig. 7b). The ΔTAD mutants also showed a significant increase in *mpx* and *il13*, along with a decreased expression of *il6*. In contrast, the T cell marker *cd4-1* was also increased in ΔTAD mutants compared to wild-type, while *hbba1* was significantly increased compared to both WT and KO mutants (Fig. 7b), indicating a wider disruption of hematopoiesis.

Discussion

STAT3 represents a critical transcription factor activated downstream of a myriad of important cytokine and other receptors that impact a wide range of essential cell functions [10]. This is reflected in the various diseases associated with STAT3, including enhanced activation and somatic GOF mutations observed in a variety of cancers, as well as inflammatory disorders such as rheumatoid arthritis and inflammatory bowel disease [70, 71]. In addition, germline STAT3 mutations – presumed to be LOF – have been linked to the development of autoimmunity and impaired innate immunity leading to enhanced susceptibility to infection [10, 72]. Insight from mouse models has identified key roles for STAT3 in hematopoiesis and immunity, including neutrophil and macrophage functionality [16]. However, these studies have been typically limited to specific cell lineages, resulting in a need for additional models to study STAT3 function, including mutants that contribute to disease.

The zebrafish Stat3 protein is highly conserved with mammalian STAT3 proteins, with strong sequence homology across an identical domain structure, with the zebrafish *stat3* gene located syntenically with its mammalian counterparts [73]. Zebrafish also shows distinct primitive and definitive waves of hematopoiesis like mammals [74], and possesses neutrophils and macrophages with equivalent functions [75]. Therefore, to further study the contribution of STAT3 to development and function, particularly of neutrophils and macrophages, CRISPR/Cas9 genome editing technology was utilized to create a Stat3 KO mutant that lacked all functional domains, and a Stat3 ΔTAD mutant in which only the transactivation domain and adjacent tyrosine that undergoes phosphorylation to mediate dimerization were deleted [73], similar to human LOF STAT3 [9, 10, 30]. Consistent with studies of alternative Stat3 KO zebrafish [28, 29], both the KO and ΔTAD mutants exhibit reduced survival and decreased expression of *stat3* [76], the latter presumably a result of nonsense mediated decay. The survival defect precluded analysis of adults but did allow a thorough comparison of both Stat3 mutants with WT zebrafish during the primitive and early definitive waves of hematopoiesis, including the functional analysis of larval neutrophils and macrophages.

Analysis of the Stat3 KO mutants revealed for the first time that STAT3 ablation impacts primitive hematopoiesis, with a severe reduction across early hematopoietic progenitors to myeloid and erythroid progenitors and their mature counterparts. Early definitive hematopoiesis was similarly affected, with HSCs and each of the lymphoid, myeloid, and erythroid lineages decreased. This is consistent with Stat3 activity observed within early hematopoietic tissues in zebrafish [77] and suggests a role in the early progenitor/stem cell compartment that consequently impacts the development of downstream lineages. While primitive hematopoiesis has not been

Fig. 5. Effect of Stat3 mutations on the response to LPS. Wild-type (WT: **a**, **d**, **g**, **j**), knockout (KO: **b**, **e**, **h**, **k**) and transactivation domain truncation (ΔTAD: **c**, **f**, **i**, **l**) mutant 3 dpf embryos on either the Tg(*mpx*:GFP) (**a–f**) or Tg(*mpeg1.1*:GFP) (**g**–**l**) transgenic background were left uninjected (**a–c**, **g–i**) or subjected to injection with lipopolysaccharide (LPS) (**d–f**, **j–k**) and imaged 8 h post injection showing representative images with scale bars of 100 μm. Quantitation of mpx^+ cells (**m**) and $mpeg1.1^+$ cells (**n**) showing values for individual embryos. Gene expression analysis of the indicated genes in LPS-injected WT, KO and ΔTAD embryos ($n = 6$) presented as fold-change ($\log_2$) relative to uninjected (**o**). Show mean and SEM with statistical significance indicated between genotypes (**m**, **n**) or compared to WT (**o**) (***$p < 0.001$, *$p < 0.05$, ns: not significant), or between uninjected and injected ($^{\#\#}p < 0.01$, $^{\#}p < 0.05$).

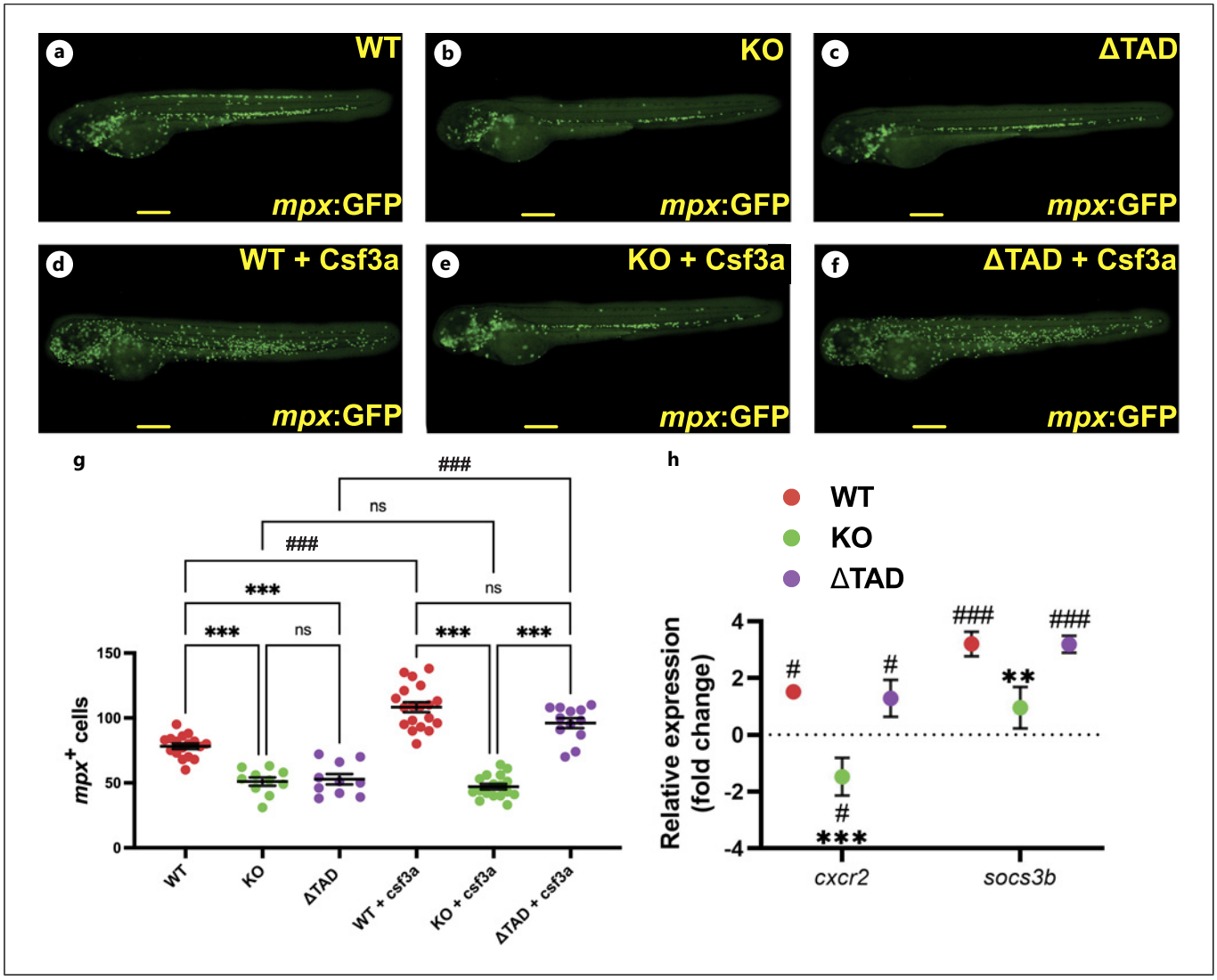

Fig. 6. Effect of Stat3 mutations on the response to G-CSF. Wild-type (WT: **a**, **d**), knockout (KO: **b**, **e**) and transactivation domain truncation (ΔTAD: **c**, **f**) mutant 1 cell embryos on the Tg(*mpx*:GFP) transgenic background were left uninjected (**a–c**) or subjected to injection with mRNA encoding the zebrafish G-CSF paralogue, Csf3a, and imaged 3 days post injection showing representative images with scale bars of 100 μm. Quantitation of mpx^+ cells (**g**) showing values for individual embryos. Gene expression analysis of the indicated genes in Csf3a-injected WT, KO and ΔTAD embryos ($n = 6$) presented as fold-change ($\log_2$) relative to WT (**h**). **g**, **h** show mean and SEM with statistical significance indicated between genotypes (**g**) or compared to WT (**h**) (***$p < 0.001$, **$p < 0.01$, ns: not significant) or between uninjected and injected ($^{###}p < 0.01$, $^{##}p < 0.01$, $^{#}p < 0.05$).

studied in Stat3 KO mice, hematopoietic-specific deletion of Stat3 in mice resulted in a defect in HSC maintenance during early definitive hematopoiesis [78–81], suggesting a conserved function in this respect.

Stat3 KO mutants also failed to elicit an increase in neutrophil numbers in response to the zebrafish G-CSF paralogue Csf3a. This was consistent with STAT3 being strongly activated downstream of G-CSFR in response to G-CSF [82, 83] and mouse models in which hematopoietic specific ablation of Stat3 blocked G-CSF-mediated granulopoiesis [24, 25], while loss of the STAT3 binding site on the G-CSFR decreased basal neutrophil levels [84]. Zebrafish Stat3 KO mutants also failed to increase neutrophils in response to immune stimulation with LPS, which mirrored the results observed during bacterial infection of mice in which Stat3 was ablated in hematopoietic cells [24], with LPS shown to drive granulopoiesis at least partially through induction of G-CSF

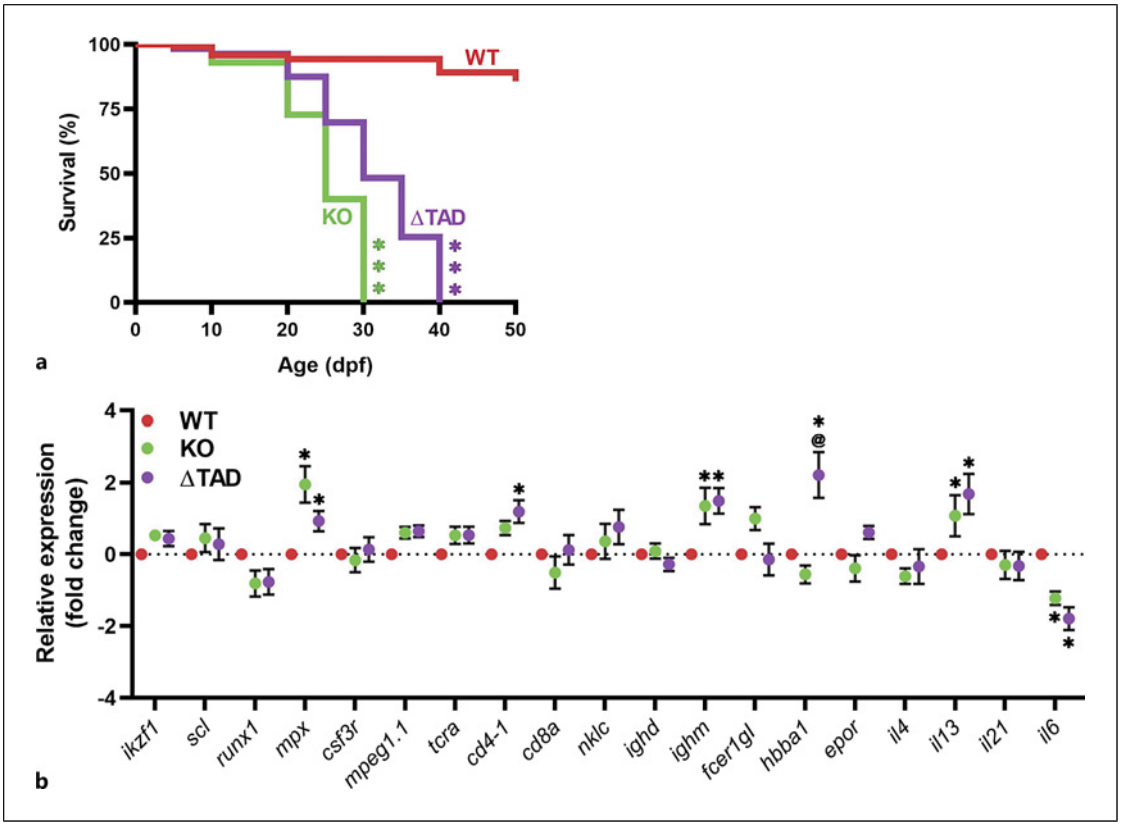

Fig. 7. Effect of Stat3 mutations on juvenile survival and immune cell development. Relative survival of wild-type (WT), knockout (KO), and transactivation domain truncation (ΔTAD) mutant zebrafish displayed as a Kaplan-Meier curve (n = 15–30) (**a**). Gene expression analysis of the indicated genes in 28 dpf WT, KO and ΔTAD juveniles (n = 6–12) showing mean and SEM (**b**). Statistical significance is indicated compared to WT (**$p < 0.01$, *$p < 0.05$) or between mutants ($^{@@}p < 0.01$, $^{@}p < 0.05$).

[85]. Collectively, this indicates a conserved role for zebrafish Stat3 downstream of its G-CSFR homolog in mediating granulopoiesis.

Neutrophils from Stat3 KO embryos were additionally impaired in their ability to be recruited in response to injury, with the rate of migration significantly diminished, but with no change in other parameters. Impaired neutrophil migration from circulation has also been observed in mice with hematopoietic-specific Stat3 ablation [60], as well as in mice expressing a G-CSFR lacking the STAT3 binding site [84]. Such migration has been shown to be primarily driven by Cxcl8 (Il-8) that acts as the main neutrophil chemoattractant via Cxcr2, with Stat3 shown to be required for both G-CSF-mediated expression of Cxcr2 [25, 60] and NF-κb-mediated expression of Cxcl8 (Il-8) [86, 87]. Long range neutrophil migration in zebrafish has been similarly demonstrated to be driven through Cxcl8 paralogues, Cxcl8a and Cxcl8b, both of which signal through Cxcr2 [44, 88], with Cxcl8b/Cxcr2 mediating neutrophil migration out of the bloodstream [44] and Cxcl8a/Cxcr2 mediating neutrophil migration towards the site of injury [43]. In addition, both Csf3b and Csf3r have also been shown to facilitate migration of zebrafish neutrophils to injury sites [41, 89]. In this study, WT zebrafish embryos showed increased expression of *cxcr2*, *cxcl8a* and *cxcl8b* in response to wounding, but this was not evident in Stat3 KO embryos despite elevated *csf3a* expression. Furthermore, Csf3a injection was unable to induce expression of *cxcr2* in Stat3 KO embryos in contrast to WT embryos. Together this suggests remarkable conservation of a G-CSF/G-CSFR/STAT3/CXCL8/CXCR2 pathway facilitating neutrophil migration. Stat3 KO mutants additionally exhibited defective neutrophil migration over the yolk during primitive hematopoiesis similar to that observed following ablation of zebrafish Csf3a [38, 41] or its receptor (Csf3r) [38, 89]. Whether this utilizes Cxcl8/Cxcr2 or another pathway remains to be determined.

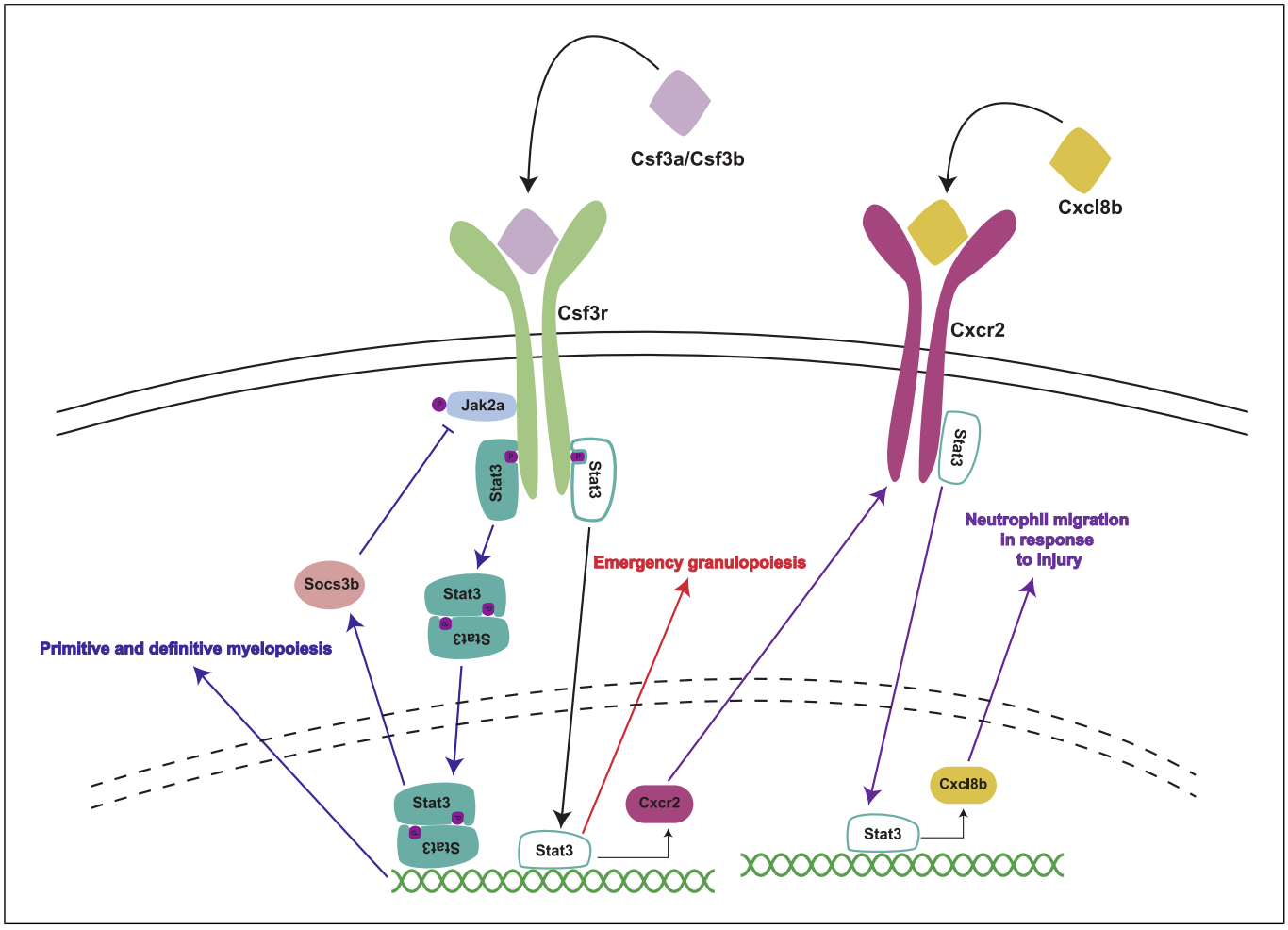

Fig. 8. Model for the role of Stat3 in the development and function of neutrophils. Schematic representation of signaling downstream of Csf3r and Cxcr2. Activation of Csf3r by either Csf3a or Csf3b induces canonical activation of Stat3 to mediate primitive and definitive granulopoiesis and is negatively regulated by Socs3b. Non-canonical Stat3 stimulated by Csf3a induces transcription of *cxcr2* to facilitate emergency granulopoiesis. Stimulation of Cxcr2 by Cxcl8b drives a positive feedback loop which increases transcription of *cxcl8b* to mediate neutrophil migration.

In contrast, relative macrophage recruitment to sites of injury was higher in Stat3 KO compared to WT embryos with macrophages also found to be significantly smaller in size in the Stat3 KO embryos suggesting an alteration in macrophage biology consistent with mouse studies that have identified roles for STAT3 in macrophage polarization and homeostasis [22]. Stat3 KO embryos also exhibited increased macrophage numbers in response to LPS. This is likely driven through Csf1a/b [59] with signaling via the CSF1 receptor not involving strong STAT3 activation [90]. Mouse models have shown that STAT3 plays an anti-inflammatory role in macrophages in response to LPS, inhibiting the activities of IL-1β, TNFα, and IFNγ; as well as stimulating the expression of SOCS3 to provide negative feedback [91, 92]. Interestingly, in this study expression of the SOCS3 paralogue *socs3b* was found to be significantly diminished in response to LPS in Stat3 KO embryos, and we have recently shown that ablation of *socs3b* induced an inflammatory macrophage phenotype [39], consistent with a role for a STAT3/SOCS3 module in controlling macrophage activation.

Despite the significantly diminished neutrophil and macrophage populations observed in their embryonic stage, during their juvenile stage the Stat3 KO zebrafish displayed elevated expression of neutrophil and other markers, indicating a rebound in cell numbers, along with elevation of the *il-13* gene, encoding a pro-inflammatory cytokine. The alternative Stat3 KO mutant produced in a previous study also

demonstrated a similar upregulation of a suite of inflammatory cytokines and chemokines [29]. We have also recently shown that both Stat3 KO and Stat3 ΔTAD mutants exhibited comparable skeletal deformities to the alternative Stat3 KO mutants, further establishing them as loss of function models [76], with no signs of compensation. Due to the similarities between these mutants and the alternative Stat3 KO mutants, it can be speculated that in addition to their skeletal abnormalities these zebrafish suffer from an immune disorder that exacerbates their poor phenotype resulting in the early lethality [29, 76]. While the Stat3 KO and Stat3 ΔTAD mutants appear to possess distinct phenotypes during their early stages, during later development their phenotypes become very similar. These phenotypes mirror those observed in global STAT3 KO mice models as they possess decreased myeloid precursor cells and an increase in neutrophils resulting in excessive inflammation [15, 84, 93].

This study utilized two Stat3 models theorizing that the Stat3 KO mutation would remove both canonical and noncanonical modes of action, but the Stat3 ΔTAD would block canonical but retain at least some noncanonical actions. Interestingly, Stat3 ΔTAD mutants displayed a range of phenotypes that both overlapped with and contrasted to those of Stat3 KO mutants. Thus, unlike Stat3 KO mutants, hematopoietic progenitor/stem cells, erythroid, and lymphoid lineages were unaffected in Stat3 ΔTAD mutants during either primitive or early definitive hematopoiesis. Instead, Stat3 ΔTAD mutants exhibited a selective reduction in neutrophil and macrophage numbers during both primitive and definitive waves, but even this was not to the same extent as Stat3 KO mutants, while the migration of neutrophils during development was also unaffected in Stat3 ΔTAD mutants. In contrast, just like Stat3 KO mutants, Stat3 ΔTAD mutants exhibited no LPS-induced increase in neutrophil numbers. However, in response to Csf3a-injection Stat3 ΔTAD mutants showed an increase in neutrophil numbers compared to Stat3 KO embryos, consistent with elevated induction of *cxcr2* and *socs3b*, as well as elevated relative neutrophil migration in response to wounding, correlating with significant upregulation of *cxcl8b* expression. Collectively, these results suggest that canonical STAT3 action is required for primitive and definitive myelopoiesis since these are impacted in both mutants. For granulopoiesis, the canonical Stat3 action is presumably mediated via Csf3r, as similar impacts were observed in zebrafish Csf3r KO mutants [89]. In addition, these activities may be negatively regulated by Socs3b (Fig. 8) since zebrafish Socs3b KO mutants displayed enhanced granulopoiesis [39], but this requires confirmation. This canonical pathway also appears to be utilized for LPS-induced granulopoiesis. The prominence of the G-CSFR/STAT3 pathway in granulopoiesis has also been demonstrated in various mice models, with similar phenotypes shown in the absence of G-CSFR and/or STAT3 [25, 84]. However, maintenance of hematopoietic progenitor/stem cells, G-CSF-mediated emergency granulopoiesis and neutrophil migration can instead be attributed to noncanonical modes of STAT3 action. Indeed, others have shown that the impacts of STAT3 on stem cell proliferation are mediated by noncanonical actions in the mitochondria [77, 94]. However, for emergency granulopoiesis and neutrophil migration the noncanonical actions appear to still rely on Csf3a/Csf3r but are independent of STAT3 tyrosine phosphorylation or TAD-mediated transcriptional activation (Fig. 8). With regard to macrophages, both canonical and noncanonical Stat3 actions appear to be involved in their regulation, although exactly which pathways they act via remains to be determined.

Disease causing STAT3 mutations have been characterized as either GOF or LOF, although it remains unclear which specific STAT3 modes of action are impacted in each scenario [10]. The most widely studied STAT3 associated disease is AD-HIES, which arises as a result of de novo germline heterozygous mutations [9, 10, 95]. While designated as LOF, many mutations fail to significantly affect STAT3 phosphorylation and/or nuclear translocation [9]. Moreover, the phenotypes of AD-HIES patients are much milder than those observed with mouse Stat3 KOs, further suggesting that not all functionality is lost [96]. The majority of AD-HIES patients suffer from eczema and recurrent Staphylococcus infections often resulting in frequent bouts of pneumonia [12], which is presumably due to impaired innate immunity, since neutrophils from AD-HIES patients have been shown to be less responsive to infections [97], and unresponsive to IL-10, resulting in increased inflammatory cytokine production [98]. More than half of AD-HIES patients also share similar skeletal and connective tissue deficiencies resulting in the development of distinct facial features [12]. A mouse transgenic model expressing an AD-HIES patient-derived mutation affecting the DNA binding domain resulted in increased susceptibility to infections [99]. The zebrafish Stat3 ΔTAD mutant has provided an opportunity to more deeply explore the innate immune deficits underpinning AD-HIES, revealing multiple deficits in neutrophil and macrophage responses. Heterozygous Stat3 ΔTAD mutants also displayed similar defects, albeit less pronounced (online suppl. Fig. 4), along with skeletal abnormalities [76], further highlighting their appropriateness as an animal model of

AD-HIES. This provides a powerful avenue to test potential therapeutics able to alleviate the various phenotypes observed in AD-HIES patients.

Acknowledgments

The authors thank staff at the Deakin University Zebrafish Facility for their excellent work maintaining the animals and Nagendra Awasthi for experimental assistance.

Statement of Ethics

This study was approved by the Deakin University Animal Ethics Committee, under project numbers: G14/2022, G15/2022, G16/2022, G23/2019, G24/2019, G25/2019.

Conflict of Interest Statement

The authors declare no conflict of interest.

Funding Sources

The research was solely funded by Deakin University, including a postgraduate stipend to MLS.

Author Contributions

Mohamed Luban Sobah designed the research, performed the research, analyzed the data, and wrote the manuscript. Clifford Liongue designed the research and analyzed the data. Alister C. Ward designed the research, analyzed the data, and wrote the manuscript. All authors contributed to editorial changes in the manuscript and read and approved the final manuscript.

Data Availability Statement

All data generated or analyzed during this study are included in this article or available upon request. Further inquiries can be directed to the corresponding author.

References

1 Levy DE, Darnell JE. Stats: transcriptional control and biological impact. Nat Rev Mol Cell Biol. 2002;3(9):651–62. https://doi.org/10.1038/nrm909.
2 Bromberg JF, Wrzeszczynska MH, Devgan G, Zhao Y, Pestell RG, Albanese C, et al. Stat3 as an oncogene. Cell. 1999;98(3):295–303. https://doi.org/10.1016/s0092-8674(00)81959-5.
3 Frank DA. STAT3 as a central mediator of neoplastic cellular transformation. Cancer Lett. 2007;251(2):199–210. https://doi.org/10.1016/j.canlet.2006.10.017.
4 Kujawski M, Kortylewski M, Lee H, Herrmann A, Kay H, Yu H. Stat3 mediates myeloid cell–dependent tumor angiogenesis in mice. J Clin Invest. 2008;118(10):3367–77. https://doi.org/10.1172/JCI35213.
5 Kortylewski M, Xin H, Kujawski M, Lee H, Liu Y, Harris T, et al. Regulation of the IL-23 and IL-12 balance by Stat3 signaling in the tumor microenvironment. Cancer Cell. 2009;15(2):114–23. https://doi.org/10.1016/j.ccr.2008.12.018.
6 Zhang L, Alizadeh D, Van Handel M, Kortylewski M, Yu H, Badie B. Stat3 inhibition activates tumor macrophages and abrogates glioma growth in mice. Glia. 2009;57(13):1458–67. https://doi.org/10.1002/glia.20863.
7 Vogel TP, Leiding JW, Cooper MA, Forbes Satter LR. STAT3 gain-of-function syndrome. Front Pediatr. 2022;10:770077. https://doi.org/10.3389/fped.2022.770077.
8 Rajala HL, Porkka K, Maciejewski JP, Loughran TP Jr, Mustjoki S. Uncovering the pathogenesis of large granular lymphocytic leukemia-novel STAT3 and STAT5b mutations. Ann Med. 2014;46(3):114–22. https://doi.org/10.3109/07853890.2014.882105.
9 Holland SM, DeLeo FR, Elloumi HZ, Hsu AP, Uzel G, Brodsky N, et al. STAT3 mutations in the hyper-IgE syndrome. N Engl J Med. 2007;357(16):1608–19. https://doi.org/10.1056/NEJMoa073687.
10 Vogel TP, Milner JD, Cooper MA. The Ying and Yang of STAT3 in human disease. J Clin Immunol. 2015;35(7):615–23. https://doi.org/10.1007/s10875-015-0187-8.
11 Zou S, Tong Q, Liu B, Huang W, Tian Y, Fu X. Targeting STAT3 in cancer immunotherapy. Mol Cancer. 2020;19(1):145. https://doi.org/10.1186/s12943-020-01258-7.
12 Tsilifis C, Freeman AF, Gennery AR. STAT3 hyper-IgE syndrome–an update and unanswered questions. J Clin Immunol. 2021;41(5):864–80. https://doi.org/10.1007/s10875-021-01051-1.
13 Al-Shaikhly T, Ochs HD. Hyper IgE syndromes: clinical and molecular characteristics. Immunol Cell Biol. 2019;97(4):368–79. https://doi.org/10.1111/imcb.12209.
14 Furtek SL, Backos DS, Matheson CJ, Reigan P. Strategies and approaches of targeting STAT3 for cancer treatment. ACS Chem Biol. 2016;11(2):308–18. https://doi.org/10.1021/acschembio.5b00945.
15 Takeda K, Noguchi K, Shi W, Tanaka T, Matsumoto M, Yoshida N, et al. Targeted disruption of the mouse Stat3 gene leads to early embryonic lethality. Proc Natl Acad Sci USA. 1997;94(8):3801–4. https://doi.org/10.1073/pnas.94.8.3801.
16 Hillmer EJ, Zhang H, Li HS, Watowich SS. STAT3 signaling in immunity. Cytokine Growth Factor Rev. 2016;31:1–15. https://doi.org/10.1016/j.cytogfr.2016.05.001.
17 Welte T, Zhang SS, Wang T, Zhang Z, Hesslein DG, Yin Z, et al. STAT3 deletion during hematopoiesis causes Crohn's disease-like pathogenesis and lethality: a critical role of STAT3 in innate immunity. Proc Natl Acad Sci USA. 2003;100(4):1879–84. https://doi.org/10.1073/pnas.0237137100.
18 Nurieva R, Yang XO, Martinez G, Zhang Y, Panopoulos AD, Ma L, et al. Essential autocrine regulation by IL-21 in the generation of inflammatory T cells. Nature. 2007;448(7152):480–3. https://doi.org/10.1038/nature05969.
19 Yang XO, Panopoulos AD, Nurieva R, Chang SH, Wang D, Watowich SS, et al. STAT3 regulates cytokine-mediated generation of inflammatory helper T cells. J Biol Chem. 2007;282(13):9358–63. https://doi.org/10.1074/jbc.C600321200.
20 Chou WC, Levy DE, Lee CK. STAT3 positively regulates an early step in B-cell development. Blood. 2006;108(9):3005–11. https://doi.org/10.1182/blood-2006-05-024430.
21 Ma CS, Avery DT, Chan A, Batten M, Bustamante J, Boisson-Dupuis S, et al. Functional STAT3 deficiency compromises the generation of human T follicular helper cells. Blood. 2012;119(17):3997–4008. https://doi.org/10.1182/blood-2011-11-392985.
22 Xia T, Zhang M, Lei W, Yang R, Fu S, Fan Z, et al. Advances in the role of STAT3 in macrophage polarization. Front Immunol. 2023;14:1160719. https://doi.org/10.3389/fimmu.2023.1160719.

23 Lee CK, Raz R, Gimeno R, Gertner R, Wistinghausen B, Takeshita K, et al. STAT3 is a negative regulator of granulopoiesis but is not required for G-CSF-dependent differentiation. Immunity. 2002;17(1):63–72. https://doi.org/10.1016/s1074-7613(02)00336-9.
24 Zhang H, Nguyen-Jackson H, Panopoulos AD, Li HS, Murray PJ, Watowich SS. STAT3 controls myeloid progenitor growth during emergency granulopoiesis. Blood. 2010;116(14):2462–71. https://doi.org/10.1182/blood-2009-12-259630.
25 Panopoulos AD, Zhang L, Snow JW, Jones DM, Smith AM, El Kasmi KC, et al. STAT3 governs distinct pathways in emergency granulopoiesis and mature neutrophils. Blood. 2006;108(12):3682–90. https://doi.org/10.1182/blood-2006-02-003012.
26 Awasthi N, Liongue C, Ward AC. STAT proteins: a kaleidoscope of canonical and non-canonical functions in immunity and cancer. J Hematol Oncol. 2021;14(1):198. https://doi.org/10.1186/s13045-021-01214-y.
27 Oates AC, Wollberg P, Pratt SJ, Paw BH, Johnson SL, Ho RK, et al. Zebrafish stat3 is expressed in restricted tissues during embryogenesis and stat1 rescues cytokine signaling in a STAT1-deficient human cell line. Dev Dyn. 1999;215(4):352–70. https://doi.org/10.1002/(SICI)1097-0177(199908)215:4<352::AID-AJA7>3.0.CO;2-J.
28 Liu Y, Sepich DS, Solnica-Krezel L. Stat3/Cdc25a-dependent cell proliferation promotes embryonic axis extension during zebrafish gastrulation. PLoS Genet. 2017;13(2):e1006564. https://doi.org/10.1371/journal.pgen.1006564.
29 Xiong S, Wu J, Jing J, Huang P, Li Z, Mei J, et al. Loss of stat3 function leads to spine malformation and immune disorder in zebrafish. Sci Bull. 2017;62(3):185–96. https://doi.org/10.1016/j.scib.2017.01.008.
30 de Araujo ED, Orlova A, Neubauer HA, Bajusz D, Seo HS, Dhe-Paganon S, et al. Structural implications of STAT3 and STAT5 SH2 domain mutations. Cancers. 2019;11(11):1757. https://doi.org/10.3390/cancers11111757.
31 Renshaw SA, Loynes CA, Trushell DM, Elworthy S, Ingham PW, Whyte MK. A transgenic zebrafish model of neutrophilic inflammation. Blood. 2006;108(13):3976–8. https://doi.org/10.1182/blood-2006-05-024075.
32 Ellett F, Pase L, Hayman JW, Andrianopoulos A, Lieschke GJ. mpeg1 promoter transgenes direct macrophage-lineage expression in zebrafish. Blood. 2011;117(4):e49–56. https://doi.org/10.1182/blood-2010-10-314120.
33 Labun K, Montague TG, Krause M, Torres Cleuren YN, Tjeldnes H, Valen E. CHOPCHOP v3: expanding the CRISPR web toolbox beyond genome editing. Nucleic Acids Res. 2019;47(W1):W171–4. https://doi.org/10.1093/nar/gkz365.
34 Hwang WY, Fu Y, Reyon D, Maeder ML, Tsai SQ, Sander JD, et al. Efficient genome editing in zebrafish using a CRISPR-Cas system. Nat Biotechnol. 2013;31(3):227–9. https://doi.org/10.1038/nbt.2501.
35 Xing L, Quist TS, Stevenson TJ, Dahlem TJ, Bonkowsky JL. Rapid and efficient zebrafish genotyping using PCR with high-resolution melt analysis. J Vis Exp. 2014(84):e51138. https://doi.org/10.3791/51138.
36 Sanchez NE, Harty BL, O'Reilly-Pol T, Ackerman SD, Herbert AL, Holmgren M, et al. Whole genome sequencing-based mapping and candidate identification of mutations from fixed zebrafish tissue. G3. 2017;7(10):3415–25. https://doi.org/10.1534/g3.117.300212.
37 Thisse C, Thisse B. High-resolution in situ hybridization to whole-mount zebrafish embryos. Nat Protoc. 2008;3(1):59–69. https://doi.org/10.1038/nprot.2007.514.
38 Liongue C, Hall CJ, O'Connell BA, Crosier P, Ward AC. Zebrafish granulocyte colony-stimulating factor receptor signaling promotes myelopoiesis and myeloid cell migration. Blood. 2009;113(11):2535–46. https://doi.org/10.1182/blood-2008-07-171967.
39 Sobah ML, Scott AC, Laird M, Koole C, Liongue C, Ward AC. Socs3b regulates the development and function of innate immune cells in zebrafish. Front Immunol. 2023;14:1119727. https://doi.org/10.3389/fimmu.2023.1119727.
40 Lieschke GJ, Oates AC, Paw BH, Thompson MA, Hall NE, Ward A, et al. Zebrafish SPI-1 (PU.1) marks a site of myeloid development independent of primitive erythropoiesis: implications for axial patterning. Dev Biol. 2002;246(2):274–95. https://doi.org/10.1006/dbio.2002.0657.
41 Meier AB, Basheer F, Sertori R, Laird M, Liongue C, Ward AC. Granulocyte colony-stimulating factor mediated regulation of early myeloid cells in zebrafish. Front Biosci. 2022;27(4):110. https://doi.org/10.31083/j.fbl2704110.
42 Kuil LE, Oosterhof N, Ferrero G, Mikulášová T, Hason M, Dekker J, et al. Zebrafish macrophage developmental arrest underlies depletion of microglia and reveals Csf1r-independent metaphocytes. Elife. 2020;9:e53403. https://doi.org/10.7554/eLife.53403.
43 de Oliveira S, Reyes-Aldasoro CC, Candel S, Renshaw SA, Mulero V, Calado A. Cxcl8 (IL-8) mediates neutrophil recruitment and behavior in the zebrafish inflammatory response. J Immunol. 2013;190(8):4349–59. https://doi.org/10.4049/jimmunol.1203266.
44 Zuñiga-Traslaviña C, Bravo K, Reyes AE, Feijóo CG. Cxcl8b and Cxcr2 regulate neutrophil migration through bloodstream in zebrafish. J Immunol Res. 2017;2017:6530531. https://doi.org/10.1155/2017/6530531.
45 Moore FE, Garcia EG, Lobbardi R, Jain E, Tang Q, Moore JC, et al. Single-cell transcriptional analysis of normal, aberrant, and malignant hematopoiesis in zebrafish. J Exp Med. 2016;213(6):979–92. https://doi.org/10.1084/jem.20152013.
46 Sertori R, Jones R, Basheer F, Rivera L, Dawson S, Loke S, et al. Generation and characterization of a zebrafish IL-2Rγc SCID model. Int J Mol Sci. 2022;23(4):2385. https://doi.org/10.3390/ijms23042385.
47 Rao X, Huang X, Zhou Z, Lin X. An improvement of the 2(-delta delta CT) method for quantitative real-time polymerase chain reaction data analysis. Biostat Bioinforma Biomath. 2013;3(3):71–85.
48 Buchan KD, Prajsnar TK, Ogryzko NV, de Jong NWM, van Gent M, Kolata J, et al. A transgenic zebrafish line for in vivo visualisation of neutrophil myeloperoxidase. PLoS One. 2019;14(4):e0215592. https://doi.org/10.1371/journal.pone.0215592.
49 Dooley KA, Davidson AJ, Zon LI. Zebrafish scl functions independently in hematopoietic and endothelial development. Dev Biol. 2005;277(2):522–36. https://doi.org/10.1016/j.ydbio.2004.09.004.
50 Kobayashi M, Nishikawa K, Yamamoto M. Hematopoietic regulatory domain of gata1 gene is positively regulated by GATA1 protein in zebrafish embryos. Development. 2001;128(12):2341–50. https://doi.org/10.1242/dev.128.12.2341.
51 Brownlie A, Hersey C, Oates AC, Paw BH, Falick AM, Witkowska HE, et al. Characterization of embryonic globin genes of the zebrafish. Dev Biol. 2003;255(1):48–61. https://doi.org/10.1016/s0012-1606(02)00041-6.
52 Lieschke GJ, Oates AC, Crowhurst MO, Ward AC, Layton JE. Morphologic and functional characterization of granulocytes and macrophages in embryonic and adult zebrafish. Blood. 2001;98(10):3087–96. https://doi.org/10.1182/blood.v98.10.3087.
53 Soza-Ried C, Hess I, Netuschil N, Schorpp M, Boehm T. Essential role of c-myb in definitive hematopoiesis is evolutionarily conserved. Proc Natl Acad Sci USA. 2010;107(40):17304–8. https://doi.org/10.1073/pnas.1004640107.
54 Willett CE, Kawasaki H, Amemiya CT, Lin S, Steiner LA. Ikaros expression as a marker for lymphoid progenitors during zebrafish development. Dev Dyn. 2001;222(4):694–8. https://doi.org/10.1002/dvdy.1223.
55 Willett CE, Cherry JJ, Steiner LA. Characterization and expression of the recombination activating genes (rag1 and rag2) of zebrafish. Immunogenetics. 1997;45(6):394–404. https://doi.org/10.1007/s002510050221.
56 Danilova N, Hohman VS, Sacher F, Ota T, Willett CE, Steiner LA. T cells and the thymus in developing zebrafish. Dev Comp Immunol. 2004;28(7–8):755–67. https://doi.org/10.1016/j.dci.2003.12.003.
57 Oehlers SHB, Flores MV, Hall CJ, O'Toole R, Swift S, Crosier KE, et al. Expression of zebrafish cxcl8 (interleukin-8) and its receptors during development and in response to immune stimulation. Dev Comp Immunol. 2010;34(3):352–9. https://doi.org/10.1016/j.dci.2009.11.007.
58 Varela M, Dios S, Novoa B, Figueras A. Characterisation, expression and ontogeny of interleukin-6 and its receptors in zebrafish (Danio rerio). Dev Comp Immunol. 2012;37(1):97–106. https://doi.org/10.1016/j.dci.2011.11.004.

59 Hason M, Mikulasova T, Machoňová O, Pombinho A, Van Ham T, Irion U, et al. SFR/CSF1R signaling regulates myeloid fates in zebrafish via distinct action of its receptors and ligands. Blood Adv. 2022; 6(5):1474–88. https://doi.org/10.1182/bloodadvances.2021005459.
60 Nguyen-Jackson H, Panopoulos AD, Zhang H, Li HS, Watowich SS. STAT3 controls the neutrophil migratory response to CXCR2 ligands by direct activation of G-CSF–induced CXCR2 expression and via modulation of CXCR2 signal transduction. Blood. 2010;115(16): 3354–63. https://doi.org/10.1182/blood-2009-08-240317.
61 Danilova N, Steiner LA. B cells develop in the zebrafish pancreas. Proc Natl Acad Sci USA. 2002;99(21):13711–6. https://doi.org/10.1073/pnas.212515999.
62 Sood R, English MA, Belele CL, Jin H, Bishop K, Haskins R, et al. Development of multilineage adult hematopoiesis in the zebrafish with a runx1 truncation mutation. Blood. 2010; 115(14):2806–9. https://doi.org/10.1182/blood-2009-08-236729.
63 Zhang Y, Wiest DL. Using the zebrafish model to study T cell development. Methods Mol Biol. 2016;1323:273–92. https://doi.org/10.1007/978-1-4939-2809-5_22.
64 Wang Z, Wu Y, Hu Q, Li Y. Differences on the biological function of three Ig isotypes in zebrafish: a gene expression profile. Fish Shellfish Immunol. 2015;44(1):283–6. https://doi.org/10.1016/j.fsi.2015.02.030.
65 Da'as S, Teh EM, Dobson JT, Nasrallah GK, McBride ER, Wang H, et al. Zebrafish mast cells possess an FcεRI-like receptor and participate in innate and adaptive immune responses. Dev Comp Immunol. 2011;35(1):125–34. https://doi.org/10.1016/j.dci.2010.09.001.
66 Paffett-Lugassy N, Hsia N, Fraenkel PG, Paw B, Leshinsky I, Barut B, et al. Functional conservation of erythropoietin signaling in zebrafish. Blood. 2007;110(7):2718–26. https://doi.org/10.1182/blood-2006-04-016535.
67 Bottiglione F, Dee CT, Lea R, Zeef LAH, Badrock AP, Wane M, et al. Zebrafish IL-4-like cytokines and IL-10 suppress Inflammation but only IL-10 Is essential for gill homeostasis. J Immunol. 2020;205(4):994–1008. https://doi.org/10.4049/jimmunol.2000372.
68 Hernández PP, Strzelecka PM, Athanasiadis EI, Hall D, Robalo AF, Collins CM, et al. Single-cell transcriptional analysis reveals ILC-like cells in zebrafish. Sci Immunol. 2018;3(29):eaau5265. https://doi.org/10.1126/sciimmunol.aau5265.
69 Bei JX, Suetake H, Araki K, Kikuchi K, Yoshiura Y, Lin HR, et al. Two interleukin (IL)-15 homologues in fish from two distinct origins. Mol Immunol. 2006;43(7):860–9. https://doi.org/10.1016/j.molimm.2005.06.040.
70 Huynh J, Chand A, Gough D, Ernst M. Therapeutically exploiting STAT3 activity in cancer–using tissue repair as a road map. Nat Rev Cancer. 2019;19(2):82–96. https://doi.org/10.1038/s41568-018-0090-8.
71 Rébé C, Ghiringhelli F. STAT3, a master regulator of anti-tumor immune response. Cancers. 2019;11(9):1280. https://doi.org/10.3390/cancers11091280.
72 Carow B, Rottenberg ME. SOCS3, a major regulator of infection and inflammation. Front Immunol. 2014;5:58. https://doi.org/10.3389/fimmu.2014.00058.
73 Yamashita S, Miyagi C, Carmany-Rampey A, Shimizu T, Fujii R, Schier AF, et al. Stat3 controls cell movements during zebrafish gastrulation. Dev Cell. 2002;2(3):363–75. https://doi.org/10.1016/s1534-5807(02)00126-0.
74 Rasighaemi P, Basheer F, Liongue C, Ward AC. Zebrafish as a model for leukemia and other hematopoietic disorders. J Hematol Oncol. 2015;8:29. https://doi.org/10.1186/s13045-015-0126-4.
75 Rosowski EE. Determining macrophage versus neutrophil contributions to innate immunity using larval zebrafish. Dis Model Mech. 2020;13(1):dmm041889. https://doi.org/10.1242/dmm.041889.
76 Sobah ML, Liongue C, Ward AC. Contribution of signal transducer and activator of transcription 3 (STAT3) to bone development and repair. Int J Mol Sci. 2023;25(1): 389. https://doi.org/10.3390/ijms25010389.
77 Peron M, Dinarello A, Meneghetti G, Martorano L, Facchinello N, Vettori A, et al. The stem-like Stat3-responsive cells of zebrafish intestine are Wnt/β-catenin dependent. Development. 2020;147(12):dev188987. https://doi.org/10.1242/dev.188987.
78 Raz R, Lee CK, Cannizzaro LA, d'Eustachio P, Levy DE. Essential role of STAT3 for embryonic stem cell pluripotency. Proc Natl Acad Sci USA. 1999;96(6):2846–51. https://doi.org/10.1073/pnas.96.6.2846.
79 Carbognin E, Betto RM, Soriano ME, Smith AG, Martello G. Stat3 promotes mitochondrial transcription and oxidative respiration during maintenance and induction of naive pluripotency. EMBO J. 2016;35(6):618–34. https://doi.org/10.15252/embj.201592629.
80 Mantel C, Messina-Graham S, Moh A, Cooper S, Hangoc G, Fu XY, et al. Mouse hematopoietic cell-targeted STAT3 deletion: stem/progenitor cell defects, mitochondrial dysfunction, ROS overproduction, and a rapid aging-like phenotype. Blood. 2012; 120(13):2589–99. https://doi.org/10.1182/blood-2012-01-404004.
81 Matsuda T, Nakamura T, Nakao K, Arai T, Katsuki M, Heike T, et al. STAT3 activation is sufficient to maintain an undifferentiated state of mouse embryonic stem cells. EMBO J. 1999;18(15):4261–9. https://doi.org/10.1093/emboj/18.15.4261.
82 Ward AC, Hermans MH, Smith L, van Aesch YM, Schelen AM, Antonissen C, et al. Tyrosine-dependent and -independent mechanisms of STAT3 activation by the human granulocyte colony-stimulating factor (G-CSF) receptor are differentially utilized depending on G-CSF concentration. Blood. 1999;93(1):113–24. https://doi.org/10.1182/blood.v93.1.113.401k33_113_124.
83 Chakraborty A, Tweardy DJ. Stat3 and G-CSF-induced myeloid differentiation. Leuk Lymphoma. 1998;30(5–6):433–42. https://doi.org/10.3109/10428199809057555.
84 McLemore ML, Grewal S, Liu F, Archambault A, Poursine-Laurent J, Haug J, et al. STAT-3 activation is required for normal G-CSF-dependent proliferation and granulocytic differentiation. Immunity. 2001;14(2):193–204. https://doi.org/10.1016/s1074-7613(01)00101-7.
85 Barreda DR, Hanington PC, Belosevic M. Regulation of myeloid development and function by colony stimulating factors. Dev Comp Immunol. 2004;28(5):509–54. https://doi.org/10.1016/j.dci.2003.09.010.
86 Grabner B, Schramek D, Mueller KM, Moll HP, Svinka J, Hoffmann T, et al. Disruption of STAT3 signalling promotes KRAS-induced lung tumorigenesis. Nat Commun. 2015;6(1): 6285. https://doi.org/10.1038/ncomms7285.
87 Zhang S, Hwaiz R, Luo L, Herwald H, Thorlacius H. STAT3-dependent CXC chemokine formation and neutrophil migration in streptococcal M1 protein-induced acute lung inflammation. Am J Physiol Lung Cell Mol Physiol. 2015;308(11):L1159–67. https://doi.org/10.1152/ajplung.00324.2014.
88 Deng Q, Sarris M, Bennin DA, Green JM, Herbomel P, Huttenlocher A. Localized bacterial infection induces systemic activation of neutrophils through Cxcr2 signaling in zebrafish. J Leukoc Biol. 2013;93(5):761–9. https://doi.org/10.1189/jlb.1012534.
89 Basheer F, Rasighaemi P, Liongue C, Ward AC. Zebrafish granulocyte colony-stimulating factor receptor maintains neutrophil number and function throughout the life span. Infect Immun. 2019;87(2):e00793-18. https://doi.org/10.1128/IAI.00793-18.
90 Stanley ER, Chitu V. CSF-1 receptor signaling in myeloid cells. Cold Spring Harb Perspect Biol. 2014;6(6):a021857. https://doi.org/10.1101/cshperspect.a021857.
91 Bode JG, Nimmesgern A, Schmitz J, Schaper F, Schmitt M, Frisch W, et al. LPS and TNFalpha induce SOCS3 mRNA and inhibit IL-6-induced activation of STAT3 in macrophages. FEBS Lett. 1999;463(3):365–70. https://doi.org/10.1016/s0014-5793(99)01662-2.
92 Bode JG, Ehlting C, Häussinger D. The macrophage response towards LPS and its control through the p38MAPK–STAT3 axis. Cell Signal. 2012;24(6):1185–94. https://doi.org/10.1016/j.cellsig.2012.01.018.
93 Chapman RS, Lourenco PC, Tonner E, Flint DJ, Selbert S, Takeda K, et al. Suppression of epithelial apoptosis and delayed mammary gland involution in mice with a conditional knockout of Stat3. Genes Dev. 1999;13(19): 2604–16. https://doi.org/10.1101/gad.13.19.2604.

94 Peron M, Dinarello A, Meneghetti G, Martorano L, Betto RM, Facchinello N, et al. Y705 and S727 are required for the mitochondrial import and transcriptional activities of STAT3, and for regulation of stem cell proliferation. Development. 2021;148(17):dev199477. https://doi.org/10.1242/dev.199477.
95 Minegishi Y, Saito M, Tsuchiya S, Tsuge I, Takada H, Hara T, et al. Dominant-negative mutations in the DNA-binding domain of STAT3 cause hyper-IgE syndrome. Nature. 2007;448(7157):1058–62. https://doi.org/10.1038/nature06096.
96 Mackie J, Ma CS, Tangye SG, Guerin A. The ups and downs of STAT3 function: too much, too little and human immune dysregulation. Clin Exp Immunol. 2023;212(2):107–16. https://doi.org/10.1093/cei/uxad007.
97 Farmand S, Kremer B, Häffner M, Pütsep K, Bergman P, Sundin M, et al. Eosinophilia and reduced STAT3 signaling affect neutrophil cell death in autosomal-dominant hyper-IgE syndrome. Eur J Immunol. 2018;48(12):1975–88. https://doi.org/10.1002/eji.201847650.
98 Giacomelli M, Tamassia N, Moratto D, Bertolini P, Ricci G, Bertulli C, et al. SH2-domain mutations in STAT3 in hyper-IgE syndrome patients result in impairment of IL-10 function. Eur J Immunol. 2011;41(10):3075–84. https://doi.org/10.1002/eji.201141721.
99 Steward-Tharp SM, Laurence A, Kanno Y, Kotlyar A, Villarino AV, Sciume G, et al. A mouse model of HIES reveals pro- and anti-inflammatory functions of STAT3. Blood. 2014;123(19):2978–87. https://doi.org/10.1182/blood-2013-09-523167.